DOI: 10.15587/978-617-7319-63-3.CH3

Volodymyr Khomenko, Oksana Chernysh, Viacheslav Barsukov,
Viktor Tverdokhlib, Arkadij Berezovskij, Volodymyr Slobodianyk

CHAPTER 3

COMPOSITE MATERIALS BASED ON WATER-SOLUBLE BINDERS FOR ELECTROCHEMICAL CAPACITORS

ABSTRACT

Today, more and more attention is paid to non-traditional rechargeable sources of electric current, which are able to quickly charge and discharge (in a few seconds or minutes), have high power (kW/kg) and a long service life (tens of thousands of charge-discharge cycles). Such current sources include electrochemical capacitors (EC), which in the special literature are called supercapacitors, ultracapacitors, ionistors, or molecular storage devices.

The principle of operation of such current sources is based on their ability to store and release electrical energy at a given time through the internal redistribution of electrolyte ions in a double electric layer (DEL). The rate of redistribution of ions in the DEL is several orders of magnitude higher than the rate of ion transfer through the "electrode-electrolyte" phase boundary during classical redox transformations in batteries. That is why ECs are non-traditional current sources, they have significant advantages over batteries in terms of their specific power, the rate of charge-discharge processes and service life, although they are inferior to batteries in terms of their capacity and energy density. Particular attention has been paid to EC in connection with the start of production in many countries of the world of environmentally friendly cars and buses with electric motors that require high power at the time of engine start. In addition to being used in transport, ECs are widely used in military and space technology, in energy storage systems at peak loads, for regulating wind generator turbines, etc.

The production of electrochemical capacitors requires fairly large capital investments. This is due to the requirements for the environmental friendliness of the production itself, where a significant amount of costs is spent on ensuring safe working conditions for personnel, on capturing harmful substances and their disposal. That is why the issue of developing EC to reduce the cost of production through the use of new materials and the improvement of technological processes becomes especially relevant.

The main scientific research in recent years in the field of EC has been associated with the study of new electrochemical systems, electrode materials and electrolytes. To a certain, but insufficient extent, attention was also paid to the improvement of the technology of combining the active material and the current collector. Even less research work is related to the development of

environmentally friendly technologies for the production of composite active materials for capacitors, although the development of these components can potentially provide high electrical performance of capacitors and significantly reduce the cost of their production. These circumstances put forward the research and development of environmentally friendly methods for obtaining composite materials for electrochemical capacitors into the category of complex, but relevant scientific and technical problems.

KEYWORDS

Electrochemical capacitor, cellular carbonaceous material, activated carbon, graphite, polymer-carbon composite, water-based polymers.

Electrochemical capacitors (EC), compared to traditional primary and secondary current sources and electrolytic capacitors, are a relatively young type of current sources that are at the beginning of their wide practical implementation. A significant difference between the operating principle of EC and traditional CCS systems is that charge accumulation occurs in a double electric layer (**Fig. 3.1**). This makes it possible to distinguish EC into a separate class of current sources.

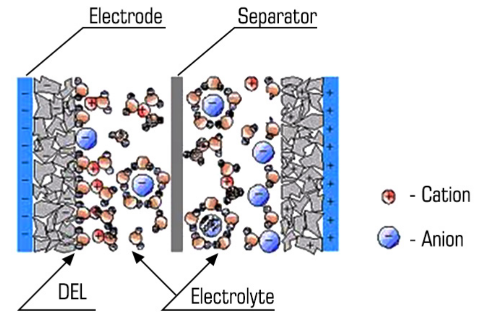

Fig. 3.1 Schematic representation of a charged EC

However, the basic principle on which the operation of EC is based remains the same as for traditional systems: a positive charge is collected mainly on one electrode, and a negative charge is collected on another, which is located nearby, but electrically separated from the first by an insulating layer. That is, the accumulation of electrical energy occurs in a static form, as in traditional capacitor systems. For EC, three main factors determining the possibility of energy storage are decisive: the surface area of the electrodes, the distance between them, and the dielectric properties of the insulating layer between the electrodes. The entire path of development of capacitor engineering was associated with the improvement of these three factors: an increase in the area of the electrodes, a decrease in the distance between them, and an improvement in the properties of the insulating layer. EC is no exception to this rule. That is, the EC capacitance is also described by the classical formula for a flat capacitor:

$$C \approx \varepsilon S / d, \tag{3.1}$$

C – EC capacitance; ε – dielectric constant of the insulating layer; S – area of the electrode; d – distance between the electrodes.

The difference is that the EC in the case of identical electrodes consists of two capacitors connected in series through the resistance of the electrolyte, where the total capacitance of the EC is described as:

$$1/C = 1/C_1 + 1/C_2, \tag{3.2}$$

and if $C_1 = C_2$, then

$$C = C_1/2. \tag{3.3}$$

According to formula (3.1), an increase in the specific area of the electrodes leads to an increase in the specific capacitance. Therefore, EC developers pay great attention to electrode materials with a large specific surface area [1].

Taking into account that the EC is actually two capacitors connected in series through the resistance of the electrolyte, the calculation of the specific capacity of the material was carried out according to the formula:

$$C_{spec} = \frac{2C_m}{T_1}, \tag{3.4}$$

where C_{spec} – specific capacity of the material; C_m – measured capacitance during discharge; T_1 – mass of the active material of one electrode.

In EC, the accumulation of electrical energy occurs directly along the electrical double layer. In this case, there is no charge transfer along the phase interface, that is, a true capacitance is observed. The surface charge generation mechanism includes surface dissociation of the electrolyte, adsorption of ions from solution in pores and defects in the electrode crystal lattice. In this case, an excess (or deficit) of charge appears on the electrode surface, and ions with the opposite charge flow around the electrode/electrolyte interface to maintain electrical neutrality [2].

The DEL thickness depends on the electrolyte concentration and ion size (**Fig. 3.2**) and is about 5–10 Å for concentrated electrolytes. The DEL capacitance varies from 10 to 20 μF/cm^2 for smooth electrodes in concentrated electrolyte solutions.

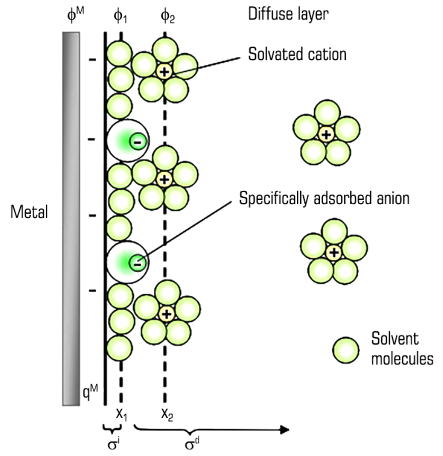

Fig. 3.2 Schematic representation of the electrical double layer

The main difference between EC and traditional electrolytic capacitors is as follows: instead of developing a microstructure (for example, increasing the surface of aluminum foil by electrochemical etching, followed by the formation of a dielectric oxide layer on it [3] with a thickness of about several micrometers), in EC, for the manufacture of electrodes, mainly carbon nanostructured materials. That is, ECs accumulate charge in carbon nanotubes or nanosized pores of activated carbon. Carbon nanofibers are used less frequently, and relatively recently information has appeared on the use of graphenes as electrode materials [4, 5].

Various names are used in the technical literature for electrochemical capacitors: ionists, supercapacitors, ultracapacitors, asymmetric capacitors, hybrid capacitors, etc. Unlike the well-known conventional capacitor, the EC does not have a dielectric layer. The technical implementation of EC began with the Baker patent (USA, 1957) [6], and its use began in the 1980s (NEC, Japan), although the basic principle was discovered at the end of the 19th century by Helmholtz [7].

Unfortunately, there is no mass production of EC in Ukraine yet. Limited Liability Company "UNASCO Ukraine", the successful scientific management of which is carried out by Corresponding Member of NAS of Ukraine, Doctor of Chemical Sciences, Yuriy Maletin, powerful ECs based on organic electrolytes were developed, which were tested in 2006 at the Institute of Transportation

Studies (Davis, CA, USA), recognized as the best among the EC prototypes of world manufacturers [8] and are now mass-produced for specific customers. It should be noted that in Ukraine there are no state programs for financing developments in the field of EC, and therefore developments are carried out through the sale of finished products. For comparison, Maxwell received 3 million USD in 2005 under the Clean Transportation Development Program in the United States for the development of EC for a hybrid bus [9].

Currently, the manufacturers mentioned above offer different types of EC, so it becomes necessary to classify them. There are different approaches to the classification of EC. The classification adopted in the USA (Miller, J., JME Inc.) [10] is generally recognized, according to which all ECs are divided into 4 classes, conventionally called generations. Each class also displays the sequence in which the given CI type appears. In accordance with the proposed classification, the following types of ECs can be distinguished:

I. *First generation ECs* contain the same positive and negative activated carbon electrodes and an aqueous electrolyte solution (mainly KOH or H_2SO_4).

II. *Second-generation ECs* are electrochemical systems similar to first-generation ECs that use an organic electrolyte based on aprotic solvents (mainly acetonitrile).

III. *Third-generation ECs* are created by combining electrodes with a fundamentally different mechanism for the occurrence of electrode reactions (charge-discharge DEL and redox process) and using an aqueous electrolyte solution. An example of such an EC is an electrochemical system in which one of the electrodes is made of activated carbon, and the second is a redox electrode made of CCS such as a nickel-cadmium or lead-acid battery.

IV. *Fourth-generation ECs* are also built using fundamentally different types of electrodes and an organic electrolyte. An example of such an EC can be electrochemical systems in which one of the electrodes is made of activated carbon, the other is made of intercalation-type materials that work inversely in aprotic electrolytes (for example, graphite or $Li_4Ti_5O_{12}$).

Third and fourth generation ECs are often referred to as "asymmetric" or "hybrid". Electrochemical capacitors can be divided into groups according to the mechanism of electrode reactions, namely:

a) EC of the electrical double layer (EC of the 1st and 2nd generation);

b) pseudocapacitive EC (3rd and 4th generations).

Accordingly, the type of electrochemical process and electrolyte are divided by the above ECs in terms of power and energy. So, ECs of the 1st, 3rd and partially 2nd generations are more powerful ECs compared to ECs of the 4th generation. The most powerful are ECs of the 1st generation (up to 15 kW/kg per pulse), but their energy does not exceed 1 Wh/kg. The most energy-intensive are ECs of the 4th generation (more than 10 Wh/kg), but their power is <1 kW/kg.

The characteristics of the above electrochemical systems depend on the method of manufacturing the electrodes. The most widely known method of manufacturing electrodes for EC is the rolling method using an aqueous suspension of polytetrafluoroethylene (PTFE) as a binder [11]. The binding mechanism is that the PTFE particles undergo fibrilization as a result of mechanical agitation and form long, thin fibers. Due to the formed fibers (fibrils), a strong electrode grid is formed. Elasticity and electrochemical stability of PTFE in a wide temperature range from –70 to +270 ^{0}C gives certain preferences to this polymeric material. In general, the rolling method has its advantages and disadvantages. The advantages of the method include the high density of the electrode and the absence of toxic organic solvents. The disadvantages of the method are the complexity of manufacturing thin electrodes (thickness less than 30 μm) and the need to preliminarily apply an adhesive sublayer to the metal current collector (most often aluminum foil), since PTFE has practically no adhesion to aluminum [12].

Carbon particles from a high electrical conductivity material are first applied to the surface of an aluminum current collector to form a carbon discrete layer. After that, an electrically conductive adhesive film is applied to the surface of the aluminum current collector formed by carbon particles, and the carbon particles are partially pressed into the surface of the polarization electrode and the aluminum current collector [13].

When carbon particles are pressed into the surface of an aluminum current collector, the oxide film on the aluminum surface is destroyed, exposing pure aluminum, while a tight mechanical contact is formed between the carbon particle and aluminum, which prevents the interaction of aluminum with oxygen in the air and the capacitor electrolyte, i.e. this ensures low resistance and stability of the electrical contact between the aluminum current collector and the particles of the carbon material pressed into its surface. The adhesive conductive film has two functions. First, it fixes the position of the polarizing electrode relative to the aluminum current collector with an embedded carbon layer, which stabilizes the operation of the electrode. Secondly, due to the electrically conductive component of the electrically conductive adhesive film, an additional electrical contact is created between the polarization electrode and the aluminum current collector, which reduces the contact resistance. Thus, the electrodes of the double electric layer capacitor, made by rolling, have a low contact resistance and high stability [14].

One of the well-known methods of manufacturing electrodes is the pressing of the active material. This method is widely used in laboratory research. For the manufacture of electrodes, activated carbon is mixed with electrically conductive additives and a polymer, followed by the formation of a mixture by pressing and heat treatment to the softening temperature of the polymer and the connection of the base with the current collector [15].

This method of manufacturing an electrode material requires the addition of a large amount of a binder material. An increase in the amount of binder leads to a decrease in the amount of activated carbon material, which significantly worsens the electrical characteristics of the capacitor. It should also be noted that this method is acceptable for the production of small-sized electrochemical capacitors with a capacity of up to 10 F [16].

The smear method [17] is well known and tested in the battery industry and makes it possible to obtain electrodes of different thicknesses – from 2 μm with an accuracy of ±1 μm [18]. The essence of the method lies in the fact that the prepared mixture of the active material with the binder solution is applied to the metal current collector, followed by drying and compaction (rolling) of the obtained active material layer. The difference in the mechanism of binding dry components in this method in comparison with the rolling method is that the binding polymers are in the state of solution, which makes it possible to more evenly distribute the polymer over the electrode volume. In addition, the range of polymers that can be used in the manufacture of electrodes is greatly expanded. Among them, the following polymeric materials should be distinguished: polyvinylidene fluoride, sodium carboxymethyl cellulose, styrene-butadiene rubber, and others [19].

Certain requirements are imposed on the polymer binder:

– inertness to electrolyte;
– high physicochemical and electrical resistance and stability;
– high adhesion to the metal down conductor;
– stability at elevated temperatures during the manufacture and operation of EC;
– high mechanical strength and elasticity of the electrode with a minimum amount of polymer in it.

All of the above requirements are met by the polymer polyvinylidene fluoride (PVDF), which is widely used in the production of chemical current sources.

The sodium salt of carboxymethyl cellulose (Na-carboxymethyl cellulose, NaCMC) is of the greatest practical importance. It is an amorphous colorless substance with a bulk density of 400–800 kg/m^3 and a density of 1.59 g/cm^3. NaCMC is an anionic polyelectrolyte, highly soluble in water. The viscosity of the NaCMC solution is practically independent of pH; it also binds water well.

Dry NaCMC salt has a weak corrosive effect. It is biologically inactive and resistant to biodegradation; however, its aqueous solutions undergo enzymatic hydrolysis during long-term storage in air (**Fig. 3.3**).

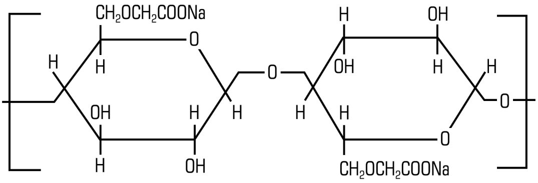

Fig. 3.3 Structural formula of the carboxymethyl cellulose sodium salt molecule

The main property of carboxymethyl cellulose is the ability to form a viscous colloidal solution that does not lose its properties for a long time [20].

It should be noted that an aqueous suspension of styrene-butadiene rubber (SBR) is used as a binder polymer, which is a completely amorphous polymer with a density of 0.91–0.99 g/cm^3 [21]. The properties of the polymer differ depending on the content of bound styrene (**Fig. 3.4**).

With an increase in the content of the attached styrene in the polymer, the density, glass transition temperature, and dielectric characteristics increase. Rubber is soluble in aliphatic and aromatic hydrocarbons, chloroform, carbon tetrachloride, carbon disulfide.

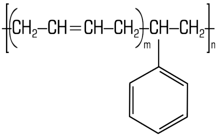

Fig. 3.4 Structural formula of styrene-butadiene rubber

3.1 RESEARCH METHODS, MATERIALS AND THEIR CHARACTERIZATION

Viscometric method

In this work, solutions of N-methylpyrrolidone with different contents of PVDF were studied. The studies were carried out using a ВПЖ-4 glass viscometer at a temperature of 30 °C, which was maintained with a thermostat.

To determine the dynamic viscosity of the studied solutions, a calibration graph (**Fig. 3.5**) was constructed based on the viscosity of glycerol solutions of different concentrations (**Table 3.1**).

Table 3.1 Viscosity and leakage time of glycerol* from the ВПЖ-4 viscometer at different temperatures

Glycerol, %	***t*, °C**	**Viscosity, cPs**	**Time, s**
100	20	1495	7286
100	25	942	4667
100	30	622	3130
95	30	248	1295
90	30	115.3	756
85	30	60	345

**Viscosity of glycerin solutions is taken from the handbook [22]*

The relative viscosity of the studied solutions was determined by the formula:

$$\eta_{spec} = \eta_{sol} \cdot \left(d_x \cdot \tau_x\right) / \left(d_{sol} \cdot \tau_{sol}\right), \tag{3.5}$$

where η_{sol} and d_{sol} – the viscosity and density of the solvent; τ_x and τ_{sol} – the outflow times of the solution and solvent, respectively; d_x – density of the solution.

The density of the solution was determined by the pycnometric method, maintaining the temperature at 30 °C.

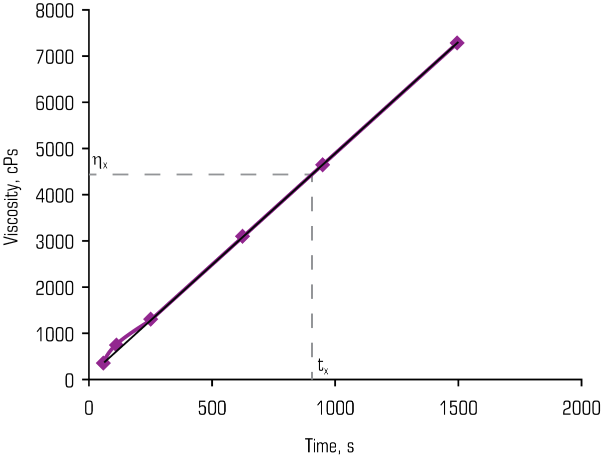

Fig. 3.5 Calibration graph

Specific viscosity reflects the increase in relative viscosity compared to unity. To take into account the influence of the concentration of the solution, it is necessary to estimate how high the specific viscosity per unit concentration of the solute is.

According to formula (3.6), the specific viscosity η_{spec} was determined:

$$\left(\eta_{spec} = \left(\eta_{s} - \eta_{sol}\right) / \eta_{sol}\right), \tag{3.6}$$

where η_{s} – viscosity of the solution; η_{sol} – viscosity of the solvent.

Formula (3.7) was used to calculate the reduced viscosity:

$$\left(\eta_{red} = \eta_{spec} / c\right), \tag{3.7}$$

where η_{spec} – specific viscosity; c – concentration of the solution.

Having plotted the graphs of the dependence of the induced viscosity on the concentration (**Fig. 3.6**), let's determine the intrinsic viscosity [η] of the solutions of the studied polymers.

For this purpose, the experimental curves were extrapolated up to their intersection with the y-axis and the numerical values of the intrinsic viscosity of PVDF solutions were determined. The characteristic viscosity does not depend on the concentration of the solution and the conformational state of the macromolecules. The dependence of intrinsic viscosity on molecular weight is described by the Mark-Kuhn-Houwink equation [23]:

$$\left[\eta\right] = \mathrm{k} \cdot M^{\alpha}, \tag{3.8}$$

where k – constant for the homologous series of polymers; α – parameter characterizing the shape of a macromolecule in solution. Its values vary within 0.55–0.85 and characterize the elasticity of macromolecule chains in solution.

The coefficients k and α are determined experimentally. From the intrinsic viscosity data, the average molecular weight of the HMC can be calculated:

$$M = \sqrt[\alpha]{\frac{[\eta]}{k}}. \tag{3.9}$$

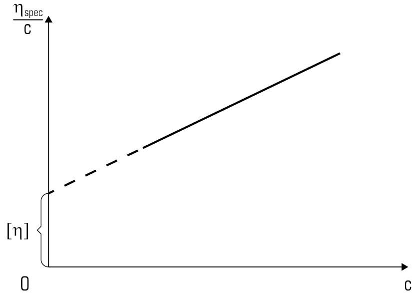

Fig. 3.6 Determination of the intrinsic viscosity of the HMC solution

Determination of viscosity by rotational method

The viscosity of the active masses during their manufacture was measured by the rotational method using the Fungilab Alpha series instrument.

Thanks to a set of rotary cylinders of different diameters, the device allows measurements in a wide range of viscosities for viscous systems, temperature range from 25 to 40 °C.

Calibration of the Fungilab Alpha series instrument was performed using silicone oil with a viscosity of 200 cSt (PMS-200, GOST 13032-77).

X-ray fluorescence analysis

To determine the chemical composition of the active masses of the electrodes, an X-Supreme 8000 X-ray fluorescence analyzer from Oxford Instruments (Great Britain) was used.

Using a spectrometer, various elements can be found from sodium to uranium. This device uses an X-ray tube with a palladium anode as a radiation source. The detector resolution is 123 eV. X-Supreme 8000 complies with international test standards such as ASTM D4294, ISO8754, ISO20847 and ISO13032.

Determination of the surface area and porosity of active masses of EC electrodes

The surface area and porosity were measured by the nitrogen capillary condensation method. Adsorption isotherms were obtained using Quantachrome Instruments version 3.0. For a detailed analysis of the porous structure of the active material of the electrode (calculation of the proportion of pores of different diameters in the total porous structure) using adsorption isotherms, the BET method proposed by Brunauer, Emmett and Taylor was used. The BET method is a method of mathematical description of physical adsorption based on the theory of polymolecular (multilayer) adsorption. The linear form of the adsorption isotherm (BET equation) has the form:

$$\frac{\rho/\rho_0}{a\left(1-\rho/\rho_0\right)}=\frac{1}{a_m C}+\frac{\left(C-1\right)\rho/\rho_0}{a_m C}, \tag{3.10}$$

where ρ/ρ_0 – ratio of the pressure in the system to the condensation pressure; a – the adsorption value; a_m – monolayer volume on the adsorbent surface; C – ratio of the adsorption equilibrium constants in the first layer and the condensation constants.

The BET method can be used to determine the surface area with an accuracy of 5–10 % in the range of relative pressure values (ρ/ρ_0) 0.05–0.35. For a more detailed analysis of the cellular structure of a solid (calculation of the proportion of pores of different diameters in the total cellular structure), additional computational models were also used from adsorption isotherms.

Infrared spectroscopy

Infrared spectroscopy was used to determine the presence of certain functional groups in polyvinylidene fluoride molecules.

IR spectra were obtained using a Termo scientific IR spectrometer, the operating range of which is within (400 cm^{-1}–4000 cm^{-1}).

In this work, we used the most common method for preparing samples for infrared spectroscopy, namely, pressing a polymer sample into a tablet with KBr.

Optical microscopy

The size and shape of particles, as well as the structure of polymers and active masses of the electrodes, were studied in direct and reflected light using microscopes MSt 30 (minor magnifications) and MB-15U42 (large magnifications, studies in penetrating and reflected light), MIN-8 (study in polarized light). The image was captured using a DCM 520 digital camera (USB 2.0). The dimensions of the structural elements were determined using an object micrometer.

Scanning electron microscopy

An electron microscope, due to its high resolution (more than two orders of magnitude higher than a light microscope), makes it possible to observe subtle features and details of the structure of micro-objects at the atomic-molecular level. The technique of scanning electron microscopy and energy dispersive elemental analysis (EDEA) was used in the work. The study was carried out on a scanning electron microscope REM-130. The EDAX EDEA detector was used to determine the elemental composition.

Method for determining the factor of structure formation

One of the most common methods for determining the structure formation factor is the "oil absorption" method. The factor is characterized by the amount of milliliters of linseed oil that is absorbed by 1 gram of soot [24].

The structure of carbon materials is understood as the type and method of combining individual particles into aggregates of larger and smaller sizes (the latter are more stable) in the form of a chain or clusters. High structure carbon materials are used to make electrically conductive plastics. Low structure – characterized by good dispersion and a slight tendency to concentrate.

On the one hand, oil claying depends on the specific surface of the particles of carbon materials, which increases with decreasing particle size; on the other hand, with the same specific surface area (and dispersion), oil absorption increases with increasing product structure. The oil absorption of different brands of carbon materials highlights the differences in their structure. Oil absorption is determined by finding the so-called points of fat content and the beginning of the flow. In the latter case, the final stage of oil absorption is reached when the so-called standing paste is formed (**Fig. 3.7, *a***), which bends to the glass plate (**Fig. 3.7, *b***) on which it was rubbed from a light push.

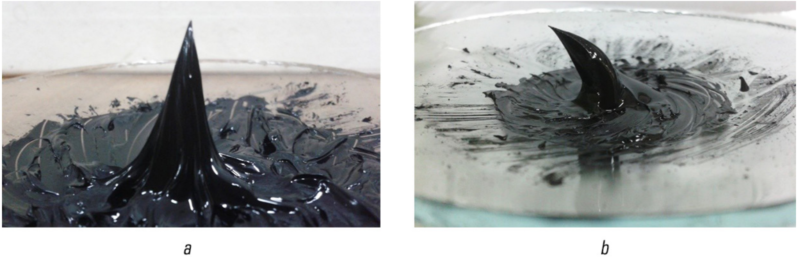
a *b*

Fig. 3.7 Image of "standing paste": *a* – an example of the existing structure of the paste; *b* – deformation of the paste during a push

The procedure itself is as follows: a 0.5 g sample of carbon material was transferred to a glass plate, to which 2 ml of linseed oil was gradually added dropwise. After each stage of adding oil, thoroughly mix the mass with a metal spatula. The final stage of oil absorption will be considered the concentration at which, after removing the spatula, the paste will be extracted into a pointed cone (**Fig. 3.7**) hence the name "standing paste".

pH determination

In the manufacture of electrodes, one has to pay attention to the interaction of the adhesive with the substrate. Not only physical interaction occurs between them, but hydrogen and even chemical bonds can form. To assess the possibility of formation of such bonds, the pH value of a solution of a polymeric aqueous extract from the corresponding carbon material is used. To do this, the investigated carbon material was boiled for several minutes, and after cooling it was filtered through filter paper. The pH value of the resulting filtrate was measured using an 801 Stirrer "Metrohm" pH meter.

Methods for determining adhesive strength

Uniform breakaway method

Particular attention was paid to the adhesion of the electrode composition to the current collector, which primarily affects the operation of electrochemical current sources. Adhesion was evaluated by the method of uniform separation of the electrode composition from the metal current collector. This method measures the amount of force applied over the entire contact area required to separate the composite polymer material from the substrate. The force is applied perpendicular to the plane of the connecting seam, and the adhesion value is characterized by the force applied per unit contact area (N/m^2) (**Fig. 3.8**).

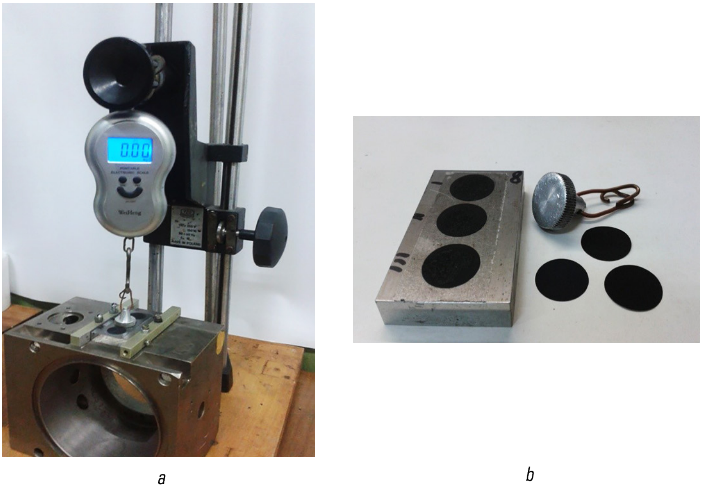
a *b*

Fig. 3.8 Laboratory unit for measuring the amount of force applied to detach the sample from the surface of the base: *a* – a device for measuring the adhesion of a composite material to a substrate; *b* – a steel plate with glued samples and a metal nickel of the same diameter, for peeling off with a load

The device consisted of a fixed platform, to which the test sample was fixed with a double-sided adhesive tape from the metal side, as well as a movable cylinder connected to an electronic dynamometer.

This movable cylinder was connected to the surface of the active layer of the electrode also by means of double-sided adhesive tape. During the study, the dynamometer together with the cylinder was slowly lifted up and the force of separation of the electrode mass from the metal current collector was recorded.

Adhesion test method using adhesive tape according to ASTM D 3359

This test procedure describes a procedure for evaluating the adhesion of coatings to metal substrates by applying and peeling off adhesive tape to slots made in the coating. A cross-shaped incision of 6 blades is made on the surface of the coating, on which the adhesive tape is glued and then torn off. Adhesion is assessed excellently on a scale from 0 to 5 (**Fig. 3.9**).

Classification	% of the removed area	Turning over sections of the grating after peeling off the tape
5B	0 % absent	
4B	< 5 %	
3B	5–15 %	 
2B	15–35 %	 
1B	35–65 %	 
0B 0B	> 65 % > 65 %	

Fig. 3.9 Classification of adhesion test results according to ASTM D 3359

However, for our coating, the qualitative assessment method was reduced to three criteria (**Fig. 3.10**):

1) good adhesion and cohesion;
2) poor adhesion, good cohesion;
3) good adhesion, poor cohesion.

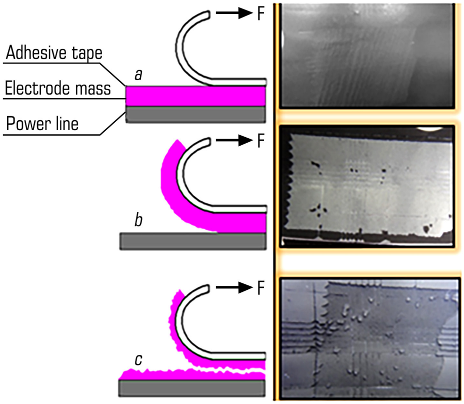

Fig. 3.10 Schematic representation of different types of destruction of the electrode layer: *a* – good adhesion and cohesion; *b* – poor adhesion, good cohesion; *c* – good adhesion, poor cohesion

Composite mixing methods

By means of an electromagnetic stirrer, mechanical mixing of the electrode mass was carried out; in some cases, heating was also used simultaneously.

A compact vacuum mixer GN-SFM-7 was also used. The mixer is designed for vacuum mixing of the components of electrode materials and obtaining homogeneous suspensions without gas bubbles.

Characteristics:

– rotation speed: not less than 320 rpm;
– ultimate vacuum: –0.8…0.9 MPa;
– vibrating platform vibration frequency: not less than 1000 Hz.

By means of ultrasonic stirring, additional dispersion of the components of the electrode mass was carried out. In addition, with the help of ultrasound, air was removed from the pores of carbonaceous materials. This method is quite effective and should not be neglected.

Method of manufacturing electrodes for EC

In the production of EC electrodes, dry substances are prepared in advance and stored in hermetically sealed containers.

Preparation of the electrode suspension is carried out by mixing the dry mixture with a certain amount of a binder solution. Preparation of the electrode mass was carried out in special mixers. Let's use the doctor blade method of applying the electrode mixture to a metal current collector (foil 20 μm thick). When applying an electrode coating on the current collector, the electrode suspension must have a certain density and viscosity, which is determined separately for each electrode composition. The electrode coating by the doctor blade method was carried out on specialized equipment such as Doctor Blade. The main instrument of this equipment was an adjustable applicator (squeegee) – a thin steel plate pointed at the end for removing the excess layer of the electrode composition. When applying the coating by the squeegee method, the electrode suspension is loaded into the applicator, which, when pulled, doses the suspension on the surface of the metal foil. The thickness of the coating layer depends on the speed of the squeegee and its distance from the surface of the foil. The quality of the coating depends to a large extent on the parameters of the application process (applicator gap distance, application speed, slurry and foil temperature) and the composition of the electrode slurry. All these parameters were optimized for each composition of the EC electrode.

After coating, the electrodes are dried in air for 20–30 min at a temperature of 60–100 °C to remove the binder polymer solvent. The final drying of the electrodes is carried out in a special vacuum cabinet at a temperature of 100–120 °C for 8–12 hours. After that, the electrodes are subjected to rolling and cutting to the standard size of the test cell.

After assembling the EC mock-ups, they were tested using electrochemical methods of analysis.

Electrochemical research methods

For various electrochemical studies, computerized potentials MSTAT 32 (Arbin Corporation, USA) and VMP3 (Princeton Applied Researcher, UK) were used.

The characteristics of electrodes and electrochemical capacitors were determined by standard methods, and the results of research and modeling were performed using specialized software for personal computers, namely:

– software for multichannel potentiostats – ARBIN (MITS Pro Software MSTAT 32, Arbin Corporation, USA) and UMP3 (EC-LAB software U9.42, Bio-Logic-Science Instruments, France);

– software for analysis and modeling of impedance spectroscopy data – ZSimpWin (Princeton Applied Researcher, UK).

Models of supercapacitors were fabricated using a sandwich cell (**Fig. 3.11**, **3.12**).

The appearance of EC layouts is shown in **Fig. 3.12**.

The EC charge/discharge characteristics at DC are produced to determine charge/discharge capacity over a specific voltage range, energy efficiency, and to calculate equivalent series resistance values.

Since the studied EC can have a wide range of capacitance values, it is necessary to set the value of the cycle current. The test current at the beginning of testing was C/1 or C/3 (where C is the rated capacitance of the EC).

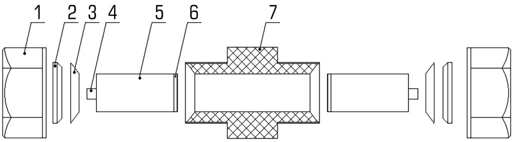

Fig. 3.11 Design of the two-electrode cell of the laboratory model of the EC: 1 – nut; 2, 3 – sealing rings; 4, 6 – down conductor; 5 – electrode; 7 – body

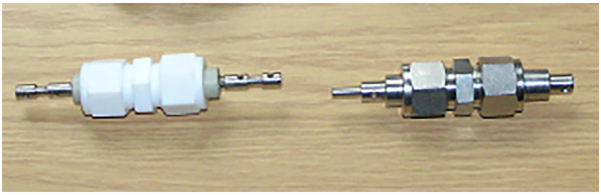

Fig. 3.12 Two-electrode laboratory mock-ups of EC

At the beginning of the test, the actual capacitance of the capacitor is unknown. Therefore, the value of the discharge current corresponding to the nominal capacity of the EC is calculated as follows. The theoretical value of the charge for the capacitor is found from the classical relation $Q=C\cdot U$ according to the equation:

$$Q=\frac{C\left(U_{\max}-U_{\min}\right)}{3600}, \tag{3.11}$$

where C – capacitance in farads; U_{max}–U_{min} – operating voltage range used in the study; Q – final charge in ampere-hours.

This Q value divided by 3 is the C/3 current rate. But the magnitude of the current is used only for the initial determination of the nominal capacity. After the test is completed and a stable capacitance is determined, the current strength is specified for subsequent testing.

Capacitor capacitance determination

The nominal capacitance was determined in a certain voltage range (from U_{max} to U_{min}) at a constant current of 5C. This value is considered more suitable for possible use in EC than C/1 or C/3 used at the beginning of testing. The nominal capacity is determined from the discharge data from U_{max} to U_{min} in 12 minutes at room temperature. The capacity of the EC is determined by the results of the discharge, which were carried out at least 3 times. The capacitance value is calculated according to the equation:

$$C_I = \frac{Q_I}{U_{\max} - U_{\min}}, \tag{3.12}$$

where C_I – actual capacitance at current I; Q_I – charge transferred at current I (in the range between U_{max} and U_{min}).

The change in nominal capacitance (ΔC) during long-term cycling was recorded as a relative value of the decrease in capacitance, expressed as a percentage of the initial capacitance C_0. Calculations are made according to the equation:

$$\Delta C(\%) = 100 \times \left(1 - C_t / C_0\right). \tag{3.13}$$

For cycling capacitors, the power loss (ΔP) and energy loss (ΔW) is calculated as a percentage of the nominal values according to equations (3.10) and (3.11):

$$\Delta P(\%) = 100 \times \left(1 - P_n^0 / P_n\right), \tag{3.14}$$

where $P_N = U^2 / 4R$;

$$\Delta W(\%) = 100 \times \left(1 - W_n^0 / W_n\right), \tag{3.15}$$

where $W_N = CU^2 / 2$.

Determination of equivalent EC resistance

The determination of the equivalent resistance RESR is made by a fixed change in the current value. The equivalent resistance is calculated according to the equation:

$$R_{ESR} = \frac{\Delta U}{\Delta I}, \tag{3.16}$$

where ΔU – change in voltage due to a change in the current value.

R_{ESR} was also determined from the data of impedance spectroscopy at a frequency of 1000 Hz.

Impedance spectroscopy

Impedance spectroscopy (IS) is used to study the metal, metal oxide or semiconductor electrode/electrolyte interface, dielectric and transport properties of materials, establish the mechanism of electrochemical reactions, study the properties of porous electrodes, passive surfaces and fuel cells, assess the state of electrochemical batteries and the integrity of poly [25–34]. The essence of the method (IS) is to apply an exciting sinusoidal signal of small amplitude to the system under study and study the signal-response caused by it at the output (**Fig. 3.13**) [35].

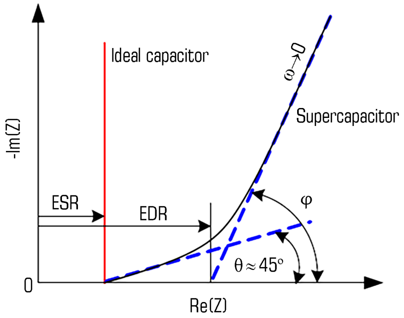

Fig. 3.13 Diffuse system resistance: (ESR) equivalent resistance – the resistance of all components of the capacitor; (EDR) equivalent diffuse resistance includes ESR and additional resistance to the process of charge redistribution in the electrode

Active materials used in the manufacture of electrodes

After preliminary studies, our attention was focused on the following carbon materials, with which the study continued (**Table 3.2**).

Table 3.2 Carbon materials with which studies were carried out

Brand	**Manufacturer**	**General information**
Supra 30	Norit (USA)	Activated carbon
Super 30	Norit (USA)	Activated carbon
Supra 50	Norit (USA)	Activated carbon
Super 30	Norit (USA)	Activated carbon
YP-50F	Kuraray Co. (Japan)	Activated carbon
Super C65	Timical (Switzerland)	Conductive additive
Pure Blake	Superior Graphite Co. (USA)	Conductive additive
Acetylene soot	MTI Co. (Korea)	Conductive additive
Carbon black-001	Superior Graphite Co. (USA)	Conductive additive
Carbon black-003	Superior Graphite Co. (USA)	Conductive additive
ABG-1000	Superior Graphite Co. (USA)	Conductive additive

Polymer binders

Among the many varieties of polymer binders, attention has been focused on N-MP-soluble polymers of polyvinylidene fluoride, as well as on its aqueous suspensions. Other water-based polymers such as polytetrafluoroethylene, styrene-butadiene rubber, and water-soluble sodium carboxymethyl cellulose were also investigated (**Table 3.3**).

Table 3.3 Characteristics of the polymeric materials used in the research

Material	Formula	Molecular weight, g/mol	Density, kg/m³	Melting point, °C
Polyvinylidene fluoride	$[-CH_2-CF_2-]_n$	90000–300000	1680–1760	171–180
Polytetra-fluoroethylene	$[-CF_2-CF_2-]_n$	140000–500000	2000–2200	326.8
Carboxymethyl cellulose sodium salt	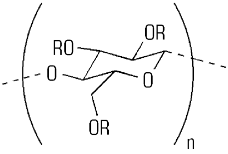 R=H or CH_2CO_2H	76000–130000	1348–1590	150–170
Styrene butadiene rubber	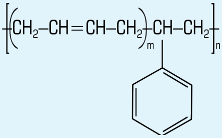 $-[(CH_2-CH=CH-CH_2)_m-CH(C_6H_5)-CH_2-]_n$	150000–400000	910–990	120–130

Materials for a metal down conductor

Since one of the important parameters of an electrochemical capacitor is the reduction of the transition resistance between the active mass and the metal current collector, various types of aluminum foil were considered (**Table 3.4**).

Table 3.4 Different types of metal down conductors

Manufacturer	Metal	Thickness, μm	Surface condition
Hohsen Co	Aluminum	20	Smooth
Kawatake Electronics Co	Aluminum	20	Etched
MTI	Aluminum	30	Applied electrically conductive carbon polymer layer
Henkel	Aluminum	30	Aqueous dispersion of LOCTITE DAG 1050 E&C graphite applied

3.2 STUDY OF POLYMERIC BINDERS

Study of physico-chemical binding properties

Today, the creation of new composite materials for EC has gained special weight, since they determine the electrical characteristics of EC. To develop modern technologies for the production of EC electrodes, it becomes necessary to choose a good polymer binder. There are certain requirements for a polymer binder that it must meet when used in chemical current sources.

One of the polymers that meets most requirements is PVDF. PVDF samples may differ in molecular weight, supramolecular structure, the introduction of another monomer units into the chain, the presence of surfactants or plasticizers. Undoubtedly, the chemical nature of the polymer binder affects its adhesion to the substrate and thus also affects the electrochemical properties of the electrode [36–39].

As part of the EU Energy Caps international collaborative project, we were tasked with researching and selecting modified PVDF polymers from Solvay's range of synthesized polymers that can be used in the manufacture of EC, and comparing their properties with some commercially available types of PVDF produced in Japan and the USA.

To evaluate the properties of PVDF, which were studied, model samples of electrodes were made containing composites based on various types of PVDF and Norit activated carbon, for which the values of the fracture force were determined by the direct separation method, as well as the surface area by the BET method. In addition, the electrodes were used to make EC mock-ups and determine internal resistances. The results obtained are presented in **Table 3.5**.

Table 3.5 Destruction strength of electrodes with different types of PVDF

Polymer code	**Without PVDF**	**Solef 0001**	**Solef 0004**	**Solef 5130**	**Solef 5320**	**Solef 6020**	**KF 1100**	**KF 9306**	**Flex 2801**
Breakaway force, N/m^2	–	680	335	860	75	225	15	1950	Peeled off
EC diffusion resistance, Ohm	–	7.6	6.7	7.8	4.1	3.9	4.4	9.2	3.7
BET surface, m^2/g	1430	830	956	850	1100	920	985	780	1150

Results in the **Table 3.5** indicate a decrease in the active surface of activated carbon when using samples of PVDF containing functional groups. Such polymer samples lead to a significant increase in the internal resistance of the EC and, accordingly, to a decrease in its power. Therefore, it is necessary to carefully optimize the content of the polymer binder in the electrode.

To establish differences in the chemical composition of PVDF samples, their IR – spectroscopic studies were carried out. **Fig. 3.14** shows the spectra of polymers Solef 6020 (curve 1) and Solef 5130 (curve 2).

The obtained IR absorption spectra indicate that the Solef 5130 polymer contains oxygen-containing functional groups. Thus, in the case of Solef 5130, intense absorption peaks appear at 1724 cm^{-1} and 1750 cm^{-1}, which can correspond to the carboxyl and carbonyl groups, respectively.

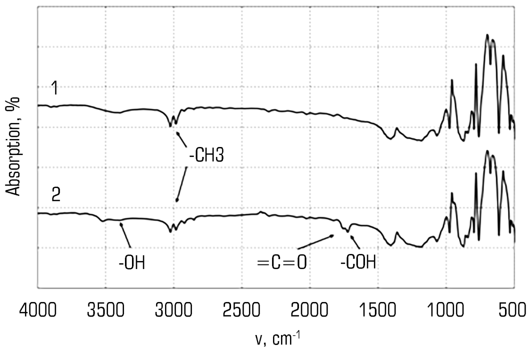

Fig. 3.14 IR absorption spectra of polymers Solef 6020 (curve 1) and Solef 5130 (curve 2)

The presence of a hydroxyl group was also established, which is confirmed by the presence of an extended peak at frequencies of 3650–3200 s^{-1}.

In this work, all selected samples of PVDF were analyzed for the presence of oxygen-containing functional groups in them. The results of IR spectroscopy are presented in **Table 3.6**.

Based on the IR spectroscopy data, all the studied samples can be divided into two groups. Solef 6020, KF 1100 and Flex 2801 polymers are functional group free. On the contrary, all other samples of PVDF (Solef 001, Solef 004, Solef 5320, Solef 5130 and KF 9306) contain functional groups in the macromolecule. It is the presence of oxygen-containing functional groups that can explain the increase in the viscosity of the polymer solution and the improvement in the adhesive properties of the metal current collector.

Reducing the amount of polymer binder leads to a decrease in adhesive properties, but increases the mass fraction of the active material. The given data indicate that different samples of PVDF provide different adhesion of the composite to the metal current collector. It can be assumed that this is primarily due to the different molecular weights of these polymers. In order to determine the molecular weight, rheological studies were carried out, the kinetic, relative, specific and intrinsic viscosities were determined, and based on the data obtained, relative viscosity versus concentration dependences were plotted. The studied solutions of PVDF with N-MP solvent were conditionally divided into low-viscosity (up to 20 Pa) (**Fig. 3.15**) and high-viscosity (up to 120 Pa) (**Fig. 3.16**).

Based on the data obtained, the intrinsic viscosity values were determined, which made it possible to determine the molecular weight of the studied PVDF using the Mark-Houwink formula (**Table 3.7**).

Table 3.6 Presence of oxygen-containing functional groups in different types of PVDF

PVDF code	**Functional group**		
	Hydroxyl (3650–3200 cm^{-1})	**Carbonyl (1750–1705 cm^{-1})**	**Carboxyl (1725–1700 cm^{-1})**
Solef 001	+	+	+
Solef 004	+	+	+
Solef 5320	+	+	–
Solef 5130	+	+	+
Solef 6020	–	–	–
KF 1100	–	–	–
KF 9306	+	+	–
Flex 2801	–	–	–

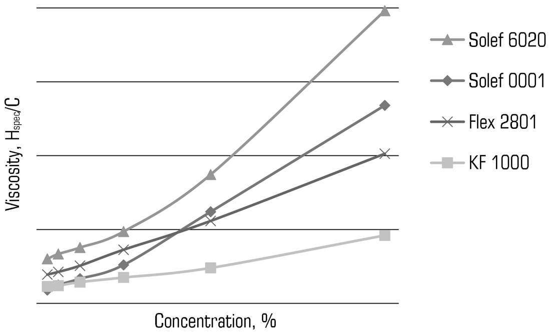

Fig. 3.15 Dependence of relative viscosity (up to 20 Pa) on the concentration of polymer binders

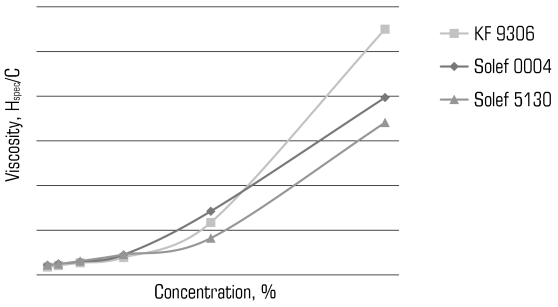

Fig. 3.16 Dependence of relative viscosity (up to 120 Pa) on the concentration of polymer binders

Table 3.7 Intrinsic viscosity and molecular weight of different types of PVDF

PVDF code	**[η] Pa·s**	**M**
Solef 001	0.710	37052
Solef 004	3.904	422727
Solef 5320	1.921	153554
Solef 5130	3.177	314944
Solef 6020	2.772	259258
KF 1100	1.067	66250
KF 9306	2.954	283938
Flex 2801	1.490	106750

Drawing an analogy between the intrinsic viscosity and the molecular weight of polymers, it can be assumed that for uniform dispersion of the active mass of the electrode and ensuring optimal physico-chemical characteristics, the best option is a viscosity within 3 Pa·s. This value corresponds to the polymers Solef 5130, Solef 6020 and KF 9306, which molecular weights are quite close in value. However, the latest KF 9306 is characterized by the fact that its working solution (5 %) has a fairly large increase in viscosity.

According to the nature of the curves in the graphs, it can be assumed that low-viscosity polymers crystallize with the formation of a spherulitic structure, while high-viscosity polymers remain with an amorphous structure. It is known that the adhesion of amorphous polymers to the substrate is preferable compared to crystallizable polymers. The best adhesion performance in our studies was demonstrated by the Kureha KF 9306 polymer. However, if we take into account the value of the useful surface area for electrodes according to the BET analysis results, then the Kureha KF 9306 polymer blocks it to the maximum. In addition, EC samples, the electrodes of which are made using this binder, have the highest resistance.

In terms of adhesive properties and molecular weight, Solef 5130 is the closest to KF 9306. Based on the results obtained, Solef 5130 and Solef 6020 were selected for further studies. Based on the dependence of viscosity on binder concentration, it can be concluded that polymers with low viscosity. (**Fig. 3.14**) refer to polymers with linear macromolecules capable of crystallization. The degree of crystallinity of the PVDF homopolymer is 60 %. While high-viscosity polymers (**Fig. 3.16**) can be attributed to typical amorphous ones by the nature of the curves. To determine the supermolecular structure of these polymers, films were formed from solutions; micrographs of their structures are shown in **Fig. 3.17**.

In **Fig. 3.17, *a*** is a micrograph of a film with Solef 6020 polymer, which crystallizes to form a typical supramolecular spherulitic structure. A micrograph for a Solef 5130 film in **Fig 3.17, *b*** indicates that the supramolecular structure is globular, characteristic of amorphous polymers.

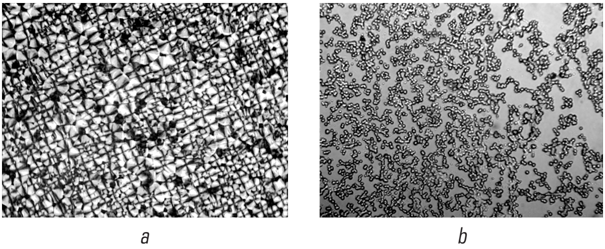

Fig. 3.17 Supermolecular structure of PVDF films: *a* – Solef 6020, magnification (x20); *b* – Solef 5130, magnification (x80)

Based on the theory of polymer adhesion, our results well confirm the fact that amorphous polymers always have preferable adhesion characteristics than crystalline ones. It is known from the literature that with an increase in the viscosity of the polymer solution, its adhesive properties decrease. But in our case, high adhesion with Solef 5130, in theory, is facilitated by the functional groups present in the macromolecule, which are capable of forming hydrogen, and possibly chemical bonds with oxygen groups on the metal surface.

Analyzing the results of the experiments, we can conclude that the nature of the interaction of the studied polymers with the carbon filler segments is different. If the Solef 5130 macromolecules interact better with the filler lobules, which promotes adhesion to them, then they are limited by the ability to move one relative to the other. Also, a polymer containing various functional groups can interact more strongly with the surface of the carbon material. Such an interaction can manifest itself in blocking the active surface of the electrode material, which is undesirable for EC electrodes. This conclusion was confirmed experimentally. According to (**Fig. 3.18**), it can be argued that the Solef 5130 polymer with functional groups blocks the activated carbon surface more strongly, increasing the EC diffuse resistance in the Nyquist diagram by almost a factor of two.

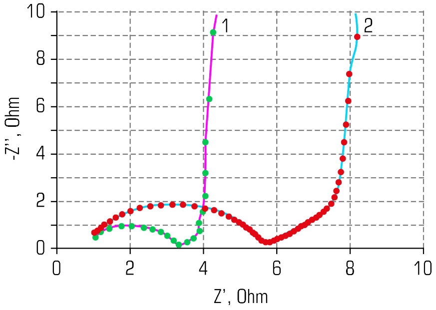

Fig. 3.18 Nyquist diagram obtained for EC with electrodes with various polymer binders: 1 – Solef 6020; 2 – Solef 5130

Effect of polymer binder concentration on electrode properties

It should be noted that the mechanical properties of electrodes largely depend on the conditions of their manufacture, as well as the ratio of components. In this paper, the physical and mechanical properties of various EC electrodes based on the use of Solef 5130 and Solef 6020 as a binder were studied. Particular attention was paid to the adhesion of the electrode composition to the current collector, since it primarily affects the operation by affecting the contact of the electrode mass with the current collector, thereby changing the contact resistance of the system. To evaluate the adhesive properties of the studied PVDF samples, electrode samples were made. Adhesion was evaluated by the method of uniform separation of the electrode composition from the metal current collector. This method measures the amount of force applied over the entire contact area, which is necessary to separate the composite polymer material from the substrate (**Table 3.8**).

⬢ **Table 3.8** Dependence of the force to destruction of the carbon composite layer on the binder concentration. (Electrode composition: Solef 6020 – 4–8 %, graphite – 89–93 % and carbon filler (graphitized carbon soot) – 3 %)

Polymer code	Binder content, %	Thickness of the wet active layer, μm	Thickness of the active layer after drying, μm	Breaking force, N/m^2
PVDF – 5130	4	100	92	2073
PVDF – 5130	6	100	81	2994
PVDF – 5130	8	100	78	3651

A decrease in the concentration of the binder in the composite material reduces its adhesion to the metal, worsens the cohesive properties of the electrode mass, brittleness appears, but the density and electrical conductivity of the electrodes increase and the content of the active material increases.

One of the main requirements for a polymer binder is to ensure sufficient mechanical strength of the electrode composite itself with its minimum amount. An increase in the polymer content in the electrode not only reduces the usable mass of the electrode, but also increases its resistance [40]. In most cases, the content of dry polymer content in the electrode should not exceed 10 %.

The influence of the binder concentration (by dry residue) on the adhesion of a composite material to an aluminum current collector was studied in this work. As can be seen from the results given in **Table 3.9**, with an increase in the content of Solef 5130 in the original composition from 4 to 8 wt. % adhesion of composites increases by 80 %.

The same pattern is observed in Solef 6020, where adhesion increased by 70 %. This is obviously caused by changes in both the composition and structure of the electrodes.

Taking into account the different viscosities of the working solutions of the studied polymers, it is obvious that the density of the electrode compositions prepared under the same conditions will be different. Samples prepared on the basis of a less viscous 5 % solution in N-MP Solef 6020 have a noticeably higher density (**Table 3.9**).

Table 3.9 Effect of PVDF content on the adhesion of electrode active material

PVDF concentration, %	PVDF concentration, %	Graphite content, %	Conductive additive, 3 %	Density ρ, kg/m^3	Breaking force, N/m^2
5130	8	89	Pure Black	946	1774
5130	6	91	Pure Black	1275	520
5130	4	93	Pure Black	1539	353
5130	8	89	C65	1414	1970
5130	6	91	C65	1688	764
5130	4	93	C65	–	412
6020	8	89	Pure Black	1235	916
6020	6	91	Pure Black	–	539
6020	4	93	Pure Black	1780	221

This is probably due to the greater mobility of the particles of the dispersed phase in the solution of this polymer in the process of applying the composite material to the current collector using the Doctor Blade device. Analyzing the results of the research, it can be concluded that with a decrease in the concentration of the binder, the density of the electrode material increases, on which the electric capacitance of the electrode depends.

3.3 EFFECT OF EC ELECTRODE MANUFACTURING CONDITIONS ON THEIR CHARACTERISTICS

We have studied the influence of such factors on the characteristics of EC electrodes:
- suspension mixing time;
- mechanical mixing and ultrasonic dispersion;
- influence of drying and rolling temperature.

Temperature-time modes of preparation of EC electrodes

The distribution of the binding volume of the composite material is undoubtedly affected by the technological parameters of their manufacture. There is a significant improvement in the adhesion of the composite (**Fig. 3.19**) to the substrate with an increase in the mixing time of the suspension used to obtain it. The combination of mechanical mixing with the use of ultrasonic dispersion of the system components improves the characteristics of the electrodes and reduces the mixing time of the suspension by 2–3 times.

Mechanical mixing with the additional action of ultrasound, in our opinion, is not only a mechanical process, since the viscosity of the system decreases with time. Composite material of long mixing is able to deform more easily under load. This can be explained by the partial destruction of macromolecules under the action of the bias voltage and the fixation of the formed radicals on the unpaired electrons of the carbon segments. Of course, the capacitance of the electrode depends on the amount of active material in it. But the existing technology practically does not allow increasing the thickness of the composite layer. With a thickness of more than 200–250 microns, when the composite dries, a system of cracks appears on its surface. This is primarily noticeable when the binder has insufficient adhesion to the filler. **Fig. 3.20** shows a photograph of the surface of a composite based on Solef 6020.

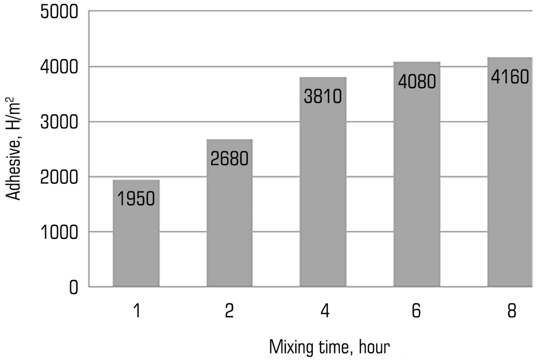

⬡ **Fig. 3.19** Dependence of the adhesive properties of the composite material on the mixing time

⬡ **Fig. 3.20** Partial destruction of the active mass during separation (layer thickness 250 μm, magnification 5x)

The formation of these cracks is facilitated by the compression of the polymer during drying. Model samples of films obtained from a solution of PVDF in N-MP showed that their shrinkage upon drying was approximately 10 % (**Fig. 3.21**) [41].

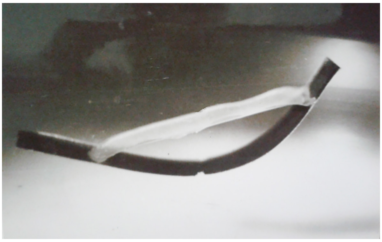

Fig. 3.21 Shrinkage of the polymer after drying

In our opinion, with high adhesion of the polymer, the active mass adjacent to the metal is not able to contract when the solvent evaporates. With distance from the adhesive layer, its influence on the counteraction of the sealing forces gradually decreases and, at a certain distance, the cohesive forces in some places are not able to withstand the stresses that arise during drying.

The effect of the adhesive layer on the mechanical properties of the electrodes is also evidenced by the results of the studies given in **Table 3.10**. With an increase in the thickness of the active mass, its mechanical properties decrease.

Table 3.10 Dependence of breakaway force on coating thickness

Thickness of the wet active layer, μm	**50**	**100**	**120**	**140**	**160**	**180**
Breakaway force, N/m^2	4700	4425	4380	4290	3985	2980

An important parameter in the manufacture of electrodes are temperature-time conditions. To assess the effect of temperature on the properties of Solef 6020 films, model samples were made from its solutions in N-MP under normal conditions. The polymer was applied to copper tapes 0.5×7 cm in size; their thickness after drying was 0.5 mm. They are elastic, easily stretched with the formation of a neck, in which the original structures turned into fibrillar. Their elongation before failure is 50–70 %. After heating the films to 150 °C (the crystallization temperature of polyvinylidene fluoride is 140–150 °C), the films become rigid and insoluble in N-MP in a short time. After a series of experiments, the drying temperature of the samples was chosen at 120 °C. The effect of the film heating time at this temperature on the adhesive properties of the polymer is shown in **Fig. 3.22**.

At the studied temperature, to relieve stress, the macromolecules gradually begin to occupy the most favorable position on the surface of the substrate over time, which contributes to an increase in adhesion.

As seen in **Fig. 3.22**, already after 120 min of warming up, the value of the load force almost does not change with time. In addition, according to the previously obtained results, it was shown that already after 180 min of heating, the density of the polymer begins to increase significantly. The results obtained showed that the maximum reverse deformations are observed in the region up to 180 min and heating at a temperature of 120 °C. The nature of residual deformation changes during heating. Vacuum-dried samples are deformed uniformly and the main type of plastic deformation is due to the movement of macromolecules relative to each other. But already in the process of heating, when the samples are stretched, "necks" appear on the material, associated with the transition of the initial globular to the oriented fibrillar structure, the reverse deformation of which does not exceed 1 % (**Fig. 3.23**).

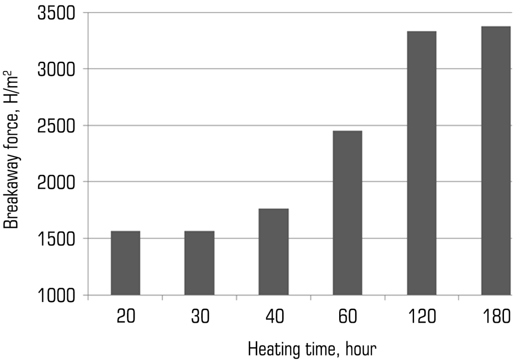

Fig. 3.22 Dependence of the breakaway force on the heating time at 120 °C

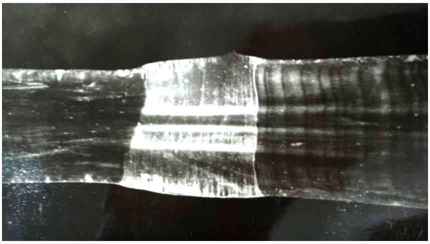

Fig. 3.23 Image of a polymer film with the "neck" formation

Thus, it can be seen from the results obtained that the main processes at the molecular level occur when PVDF is heated at 120 °C for up to 180 minutes. Further heating not only reduces the reverse deformation, but also stiffens the structure.

Electrode rolling

The specific energy consumption of EC depends on the specific mass of the active substance on the surface of the current collector. During the evaporation of the solvent, the composite material is compacted on the surface of the current collector (**Fig. 3.24**), but the lobules of the solid filler interfere with obtaining the active mass of the desired density.

It should be taken into account that the technique for the production of electrodes implies the compaction of the dried composite material using rollers at an elevated temperature (100 °C). An increase in temperature reduces the internal stress that occurs during the evaporation of the solvent, and thus increases the adhesive properties of the polymer (**Table 3.11**). It has been established that the compaction of the electrode composition improves the adhesive properties by 8–12 %.

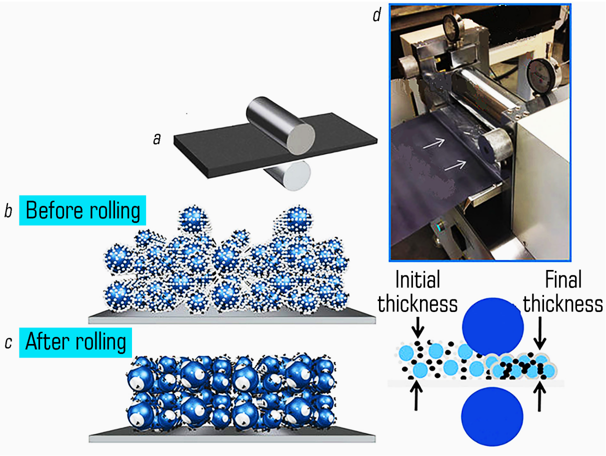

Fig. 3.24 Scheme of rolling electrodes and the device itself: *a* – rolls for rolling; *b* – electrode for rolling; *c* – electrode after rolling; *d* – device

Table 3.11 Density and breakaway force of the active layer of electrodes before and after their rolling (composite composition: graphite – 89–91 %, conductive admixture Pure Black – 3 %, binding Solef 5130 – 6–8 %)

№	PVDF, %	Before rolling		After rolling	
		ρ, kg/m^3	*P*, N/m^2	ρ, kg/m^3	*P*, N/m^2
1	8	873	2484	995	2822
2	6	977	2185	1147	2372

By means of rolling, all components of the electrode mass are compacted. This, in turn, promotes better contact between the active material and the conductive additives. Also in the work, the influence of the temperature of the rollers was studied. It has been established that heating the electrodes during rolling reduces the tension of the material itself and contributes to a more uniform and compact arrangement of the components of the electrode mass. The heating of the electrodes during compaction of the active material reduces the internal resistance of the electrode and thereby improves the electrical conductivity of the system as a whole. As can be seen from **Table 3.12**, the appearance of the surface of the electrodes without rolling and with rolling at a temperature of 100 °C differs significantly after cutting through the electrodes.

Table 3.12 Image of the surface of the electrodes after applying the method with cutting into segments. Electrode composition: activated carbon YP-5F – 89 %, conductive additive C65 – 5 %, polymer binder Solef 6020 – 6 %

Rolling	After cutting	After peeling off the tape
Without rolling	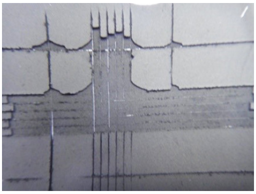	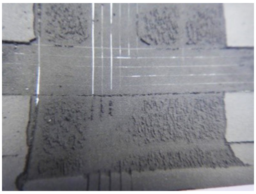
Rolling at temperature (100 °C)	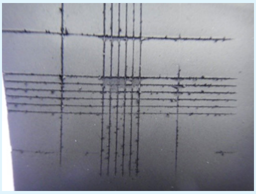	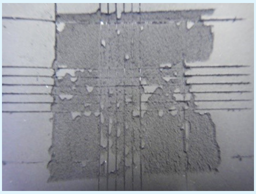

The active mass of the electrode without rolling already after cutting peels off quite easily and disappears, however, such a result is no longer observed after the application of rolling. The second stage of this experiment after peeling off the adhesive tape is characterized by better adhesion of the sample with rolling compared to the sample without rolling.

There is a direct relationship between rolling force and internal resistance - the greater the compaction, the lower the resistance. But there are reasonable limits to rolling beyond which further compaction is inappropriate. After a series of experiments, it was determined that compaction of 20–30 % of the electrode mass is optimal. With further compaction of the active layer of the electrodes, a shear stress arises (**Fig. 3.25**), which can adversely affect the structure of the composite and even deform the metal current collector (**Fig. 3.26**).

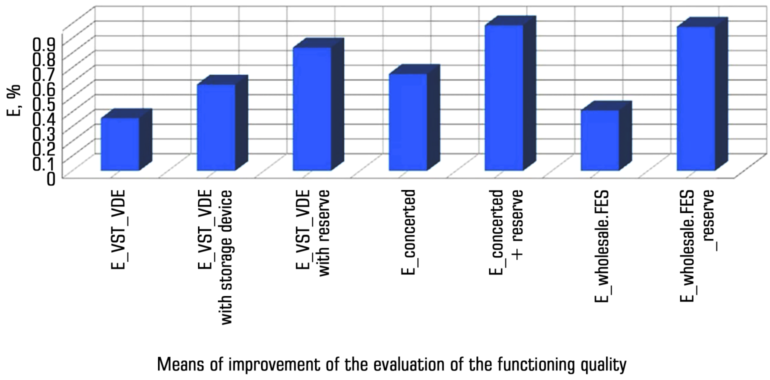

Fig. 3.25 Schematic representation of the applied load during rolling

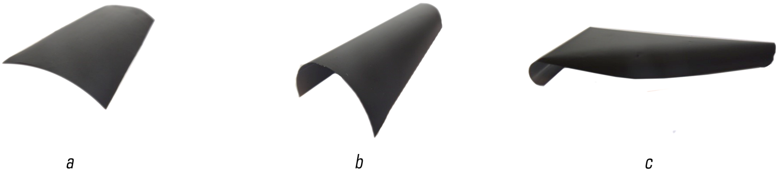

Fig. 3.26 Image of electrode deformation after sealing: *a* – sealing on 20 %; *b* – sealing on 35 %; c – sealing on 50 %

Note: Electrode composition: activated carbon (YP-50F) – 88 %, conductive additive C65 – 5 %, polymer binder Solef 6020 – 7 %

Under the action of pressure, the interlayers of the polymeric binder between the lobules of the active material decrease and the area of contacts between them increases, which, of course, contributes to a decrease in the electrical resistance of the electrodes.

Table 3.13 shows the values of the internal resistance of EC, assembled with electrodes before and after compaction.

Table 3.13 Change in the internal resistance of the EC depending on the compaction modes

PVDF type	PVDF content, %	Electrode processing	R_{ESR}, Ohm	R_{EDR}, Ohm
Solef 6020	8	Without rolling	0.28	4.85
		Rolling without heating (20–25 °C)	0.28	1.72
		Rolling at heating (100 °C)	0.27	0.59

**EC assembled on the basis of activated carbon Norit Supra 50 and electrolyte -1.5 M TEABF4 in acetonitrile, electrode area 2 cm^2*

Selection of a metal down conductor for EC

An essential component of the total resistance of the electrode is the resistance between the active mass and the metal current collector.

In this work, electrodes were fabricated using commercial samples of aluminum foil recommended for use in lithium-ion batteries (LIA) and EC. To compare adhesive and electrical characteristics, four types of aluminum current leads were selected (**Table 3.14**), namely, foils manufactured by Hohsen Co. (*a*), Kawatake Electronics Co. (*b*) LIB foil pre-coated with an electrically conductive carbon-polymer layer obtained from MTI Co. (*c*), as well as an analogue of such a composite current collector, made by applying a hydrogen dispersion of LOCTITE DAG 1050 E&C graphite to aluminum foil from Henkel (*d*). The selection of graphite dispersion LOCTITE DAG 1050 E&C is based on Henkel's recommendation of this product for the production of lithium-ion battery electrodes and electrochemical capacitors.

As can be seen from **Table 3.14**, the foil sample from Kawatake Electronics Co. has the best adhesion (breakaway force) (Japan) and a sample with a carbon-polymer layer from MTI Co. (USA), although the latter demonstrates a rather high resistance as part of the finished EC.

Table 3.14 Commercial samples of aluminum foils for use in LIB and EC*

Code	Aluminum foil (manufacturer)	Breakaway force, N/m^2	EC Resistance R_{EDR}, Ohm
(*a*)	Foil from Hohsen Co. (Japan)	3381	1.43
(*b*)	Foil from Kawatake Electronics Co. (Japan)	4704	1.15
(*c*)	Foil from MTI Co. with carbon-polymer layer (USA)	4116	4.31
(*d*)	Foil from Henkel with graphite layer LOCTITE DAG1050 E&C	1744	5.12

**EC assembled on the basis of activated carbon Norit Supra 50 and electrolyte -1.5 M TEABF4 in acetonitrile, electrode area 2 cm^2*

A sample with a carbon layer based on LOCTITE DAG1050 E&C demonstrates both sufficiently low adhesion and the highest resistance in the EC composition. This indicates that the polymer used by LOCTITE DAG1050 E&C has poorer adhesion to the Henkel foil.

We have found that the main criteria affecting the adhesion force are the surface and the shape of the aluminum foil surface relief. The more developed the surface and the inhomogeneous relief, the better the contact of the active mass of the electrode with the metal surface. This profile is achieved by targeted surface treatment of the aluminum foil by the manufacturer.

Fig. 3.27 shows the change in the EC impedance in the case of using foil from Hohsen Co. as a current collector. and Kawatake Electronics Co.

As can be seen from **Fig. 3.27**, the modification and increase in the specific surface area of the current collector (foil from Kawatake Electronics Co.) significantly reduces the internal resistance of the capacitor compared to the EC based on untreated (smooth) foil from Hohsen Co.

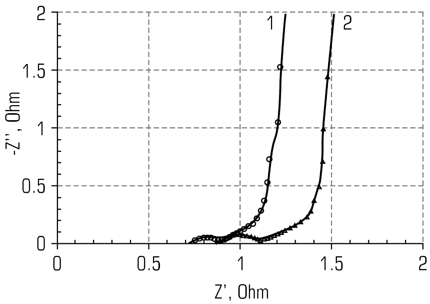

Fig. 3.27 Change in EC impedance depending on the type of current collector: curve 1 – foil from Kawatake Electronics Co.; curve 2 – foil from Hohsen Co.

Also, according to the studies, it was shown that the preliminary application of an electrically conductive polymer-carbon layer does not always improve the electrical characteristics of the EC. As can be seen from **Table 3.14**, the electrically conductive polymer-carbon layer in options (*c*), (*d*), deposited on the aluminum current collector, on the contrary, significantly increases the internal resistance of the capacitor compared to modified foil electrodes from Kawatake Electronics Co., which do not have such a layer. This can be explained by the presence of a large amount of polymer in the pre-applied layer (*c*) and insufficient adhesion in option (*d*), which leads to blocking of the charge-discharge kinetics of the EC active material.

The selection of an aluminum current collector with a fine-grained relief (for example, grass foil from Kawatake Electronics Co.) can significantly (approximately 40 %) improve the adhesion of the electrode layer by increasing the effective contact surface, as well as reduce the internal resistance of the electrochemical capacitor by 20 % to a down conductor from Hohsen Co., which is often considered "standard").

Unlike the unmodified surface of the Japanese-made foil, the surface of the Kawatake Electronics Co. foil has been artificially modified. In our opinion, this fact can be explained by photographs of the foil surfaces (**Fig. 3.28**).

Fig. 3.28, *a* shows the surface of a Japanese Hohsen foil with machining marks. The foil surface of Kawatake Electronics Co. is modified by electrochemical digestion, which greatly increases the effective surface area.

An original technique for reducing contact resistance is proposed in patents [13]. According to this technique, slices of graphite or soot are fused into the aluminum surface using electrospark technology (**Fig. 3.28**). In this case, the aluminum oxide surface layer is destroyed and is not restored further on the graphite/aluminum interface. According to this technique, the specific contact resistance decreases by two orders of magnitude.

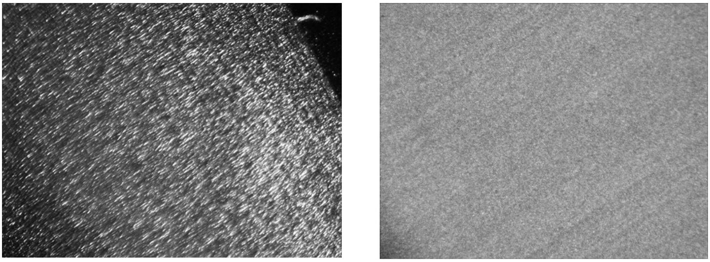

a *b*

Fig. 3.28 Surface of Al foil of the company: *a* – Hohsen; *b* – Kawatake Electronics Co.

Microscopic studies confirm the fusion of graphite particles into aluminum (**Fig. 3.29**).

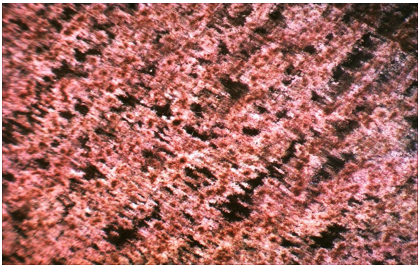

Fig. 3.29 Modified surface of aluminum foil by spark discharge

Electrospark processing leads to point deformation of the foil, which increases its specific surface.

Using the uniform breakaway method, it was determined that the adhesion of such a foil is 30 % higher compared to the adhesion of a smooth foil from Hohsen and amounted to 5580 N/m^2. However, obtaining such a foil on an industrial scale is a rather complicated process and leads to significant costs for electricity.

Thus, grass foil from Kawatake Electronics Co. shows the best results. (Japan), which has sufficiently high adhesion rates and, accordingly, a low contact resistance, which positively affects the electrochemical characteristics of EC. It was this foil that was chosen for further use in the manufacture of EC.

As a result of the studies performed, in the third chapter it can be concluded that it is the Solef 6020 polymer in N-MP that meets most of the electrochemical characteristics and requirements for a polymer binder.

The combination of mechanical mixing and ultrasonic dispersion significantly improves the homogeneity of the electrode mass suspension, which affects the uniformity of application to the metal current collector.

By many experiments, the appropriate concentrations of binder polymers, the composition of the components of the electrode mass, the thickness of the deposition, and the temperature-time modes of drying the electrodes were selected. Also, after drying the electrodes, they were additionally rolled at a temperature of 100 rolls °C for compaction. After rolling, the number of useful contacts in the electrode partially increases and, in turn, the internal resistance decreases (by 80 %). Thus, the rolling of the electrode layer improves the electrochemical and physical characteristics of the EC electrodes.

3.4 APPLICATION OF WATER-SOLUBLE POLYMER BINDERS

In further studies, the possibility of replacing the organic solvents of PVDF with water was considered. This is possible when using aqueous solutions (suspensions, emulsions) of polymers. In particular, electrodes were fabricated using mixtures of sodium carboxymethyl cellulose (NaCMC) solution with industrial acrylate (BM-12), polyurethane, and styrene-butadiene (SBR) suspensions. The active masses with these binders showed high adhesive properties of the aluminum current collector, which are not inferior to the properties of the composite based on PVDF [42].

Carboxymethyl cellulose is a simple ester of cellulose and glycolic acid [43]. It is a colorless substance, insoluble in water, low molecular weight alcohols and ketones. As a rule, not the polymer itself is used, but its sodium salt, which is also often called carboxymethyl cellulose.

NaCMC is also an amorphous colorless substance with a softening point of 170 °C and a density of 1.59 g/cm^3, soluble in water. The most common for the use of NaCMC are polymers with a degree of polymerization of 200–1500. The degree of substitution of hydroxyl groups for sodium ions in the macromolecule unit is from 0.4 to 1.2. Polymers with a degree of substitution of more than 0.4 dissolve well. Transparent solutions are characterized by high viscosity, so that the viscosity of a 2 % solution is 10–25 10^3 mPa s. NaCMC is well compatible in aqueous solutions with other water-soluble natural and synthetic polymers. In aqueous solutions, it has the properties of weak surface-active substances (surfactants). From aqueous solutions, transparent films are obtained with a breaking load of 4900–9114 N/m^2 and a relative elongation at failure of 8–14 %. Possesses weak acidic properties.

The rheological and adhesive properties of solutions of this artificial polymer depend on many factors, including the nature of the initial cellulose (cotton, wood species, and other plants), molecular weight, the degree of substitution of hydroxyl groups in the macromolecule unit, and the purity of the finished product. We had three samples of NaCMC at our disposal: technical, food (Holland), and electrolyte (Dow Chemical, Germany). In the solid state, they are in the form of a fine white powder, but their solutions are transparent. In this work, thin films formed during the drying of solutions of these polymers were carefully studied. Careful examination of these films at the optical level revealed the presence of foreign solid particles in them (**Fig. 3.30**).

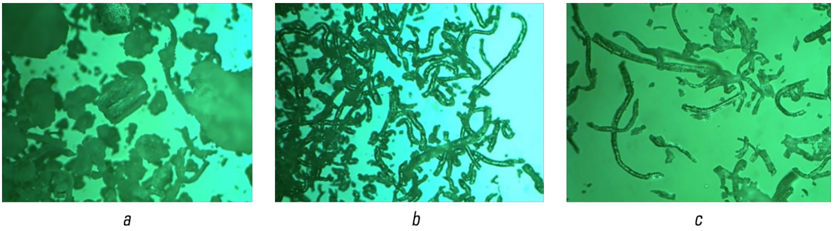

Fig. 3.30 Structure of initial NaCMC: *a* – technical; *b* – food (Holland); *c* – electrolyte (Dow Chemical, Germany)

In our opinion, wood was used as the starting material for the preparation of technical NaCMC, while residues of cotton fibers were found in the food and electrolyte samples. The conducted studies unequivocally indicate that the electrolyte NaCMC is the purest of those studied. It was this polymer that was selected for further work.

As mentioned earlier, the polymeric EC electrode binder [44] should have good adhesion to the metal current collector. Typically, in the technology of manufacturing electrodes, solutions are used, the concentrations of which are 5–8 %. It was interesting to compare the adhesive properties of 5 % solutions of PVDF and NaCMC. Thin films were fabricated from such solutions on copper foil, and after drying they were examined by the detachment method. The results show that the adhesion of PVDF (breakaway force 4537 N/m^2) is much greater (by 97 %) compared to NaCMC (breakaway force 118 N/m^2). In our opinion, this difference can be explained by a significant difference in the viscosities of the solutions studied in this experiment. Even when applying the solution to the copper base, it was clear that due to the low mobility of macromolecules in a rather viscous solution of NaCMC, the polymer wets the substrate much worse. In addition, the NaCMC viscous solution formed a thicker film compared to PVDF, which, according to theory, also weakens adhesion. To reduce the viscosity, a 1 % solution of NaCMC was prepared. The adhesion properties of such a film have increased significantly (breaking load 3676 N/m2). Considering that aqueous solutions of NaCMC are well compatible with solutions of water-soluble polymers, it was interesting to modify NaCMC with aqueous suspensions of polymers with high adhesion to metals.

Synthetic latexes are aqueous dispersions of synthetic polymers stabilized with surfactants [45]. In latex macromolecules are in the form of balls (globules). The size of the globule significantly affects the viscosity of the latex, as well as its stability. The smaller the globule size, the higher its stability. The average diameter of globules of different polymer emulsions is from 80 to 300 nm. When water-soluble polymers are added to the latex, the globules grow in size [46].

The most common are polyurethane, polybutadiene-styrene, polyacrylate synthetic latexes. An example of the globular structure of latex suspensions is shown in **Fig. 3.31**.

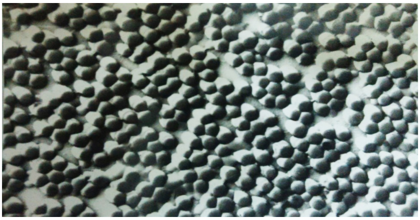

Fig. 3.31 Surface of ultrathin film of BM-12 acrylate suspension (x13000, electron microscopy)

Linear polyurethanes have the general formula $[-OCHN-R-NHCO-OR'O-]_n$.

The presence of strongly polar groups (urethane, complex and ether bonds) in the chain of the macromolecule promotes the formation of hydrogen bonds. Reactive isocyanate groups may remain at the ends of the macromolecule. There are many varieties of polyurethanes, since there are a large number of starting monomers. The disadvantage is the low resistance to thermal and thermal-oxidative degradation. Macromolecules of some polyurethanes begin to decompose at a temperature of 120 °C.

Styrene-butadiene latexes are amorphous polymers. They have a density of 0.91–0.99 g/cm^3. Soluble in aromatic and aliphatic hydrocarbons.

Polyacrylate latexes are obtained by emulsion polymerization of esters of acrylic and metaacrylic acids with different numbers of carbon atoms in the radicals [45, 46].

General formula: $(-CH_2-CR'(COOR\ -)_n$.

Physico-mechanical characteristics significantly depend on the length of the radicals. Under normal conditions, polyacrylate latexes are resistant to dilute acids and alkalis, but at temperatures above 80 °C they can be hydrolyzed by solutions of polyacrylic acid and alkalis. At temperatures above 150 °C, thermal destruction of macromolecules begins, accompanied by cross-linking of macromolecules. In this case, a slight release of monomers may occur. When the aqueous dispersion dries, polyacrylates form a stable transparent film.

Some doubts are caused by polyurethane and polyacrylate suspensions, the macromolecules of which contain active functional groups, which can later react with the components of the electrode system. Signs of the onset of coagulation were noticed when the polyacrylate suspension was added to the NaCMC solution.

For further work, preference was given to a suspension of styrene-butadiene rubber (SBR) (**Fig. 3.32**).

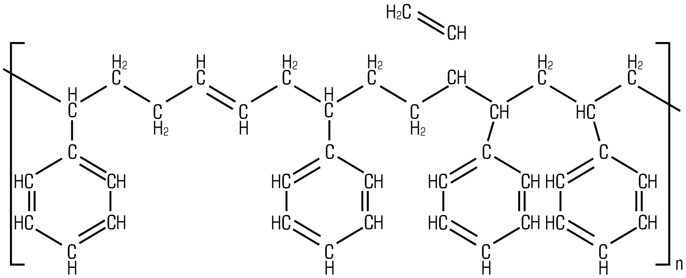

Fig. 3.32 Structural formula of styrene-butadiene rubber

First, there are no active groups in the macromolecule of this polymer that could interact with the electrolyte; the polymer is resistant to acids and bases. Secondly, the polymer has flexible chains with good adhesive properties. Thirdly, π-bonds in macromolecules and free bonds on carbon particles, under certain conditions, can lead to the formation of a cross-linked structure and, thus, strengthen the composite material. Aqueous suspension of SBR is technologically advanced, sedimentation-resistant for a long time of storage.

Thus, for further studies, a suspension of SBR was chosen for comparison and characterization.

On the basis of a mixture of NaCMC and SBR, EC electrodes were fabricated and studied. The composition of the electrode: activated carbon – 89 %, conductive additive – 5 %, polymer binder – 6 %. Table 15 shows the internal resistance values of EC based on electrodes made from these polymer binders and electrodes made from solutions of Solef 6020 in N-MP.

Table 3.15 EC internal resistance

Polymer bonding electrodes	**R_{ESR}, Ohm**	**R_{EDR}, Ohm**
NaCMC / SBR in a ratio of 1:1	1.1	2.7
Solef 6020	0.71	1.15

Electrochemical studies of electrodes based on NaCMC/SBR composites indicate their poorer stability compared to PVDF. **Fig. 3.33** shows the anodic polarization curve of an aluminum current collector, on the surface of which various polymers were deposited.

According to the results obtained, SBR can be oxidized at potentials of more than 3.7 V relative to the lithium reference electrode, which is almost 1 V less than in the case of PVDF.

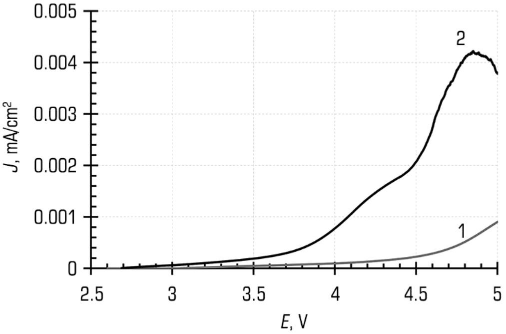

Fig. 3.33 Linear voltammetry of an aluminum current collector with a polymer film: 1 – PVDF; 2 – SBR. The potential sweep rate is 1 mV/s. Electrolyte: 1M $LiPF_6$ solution in EC/DMC (1:1)

Use of water-based polyvinylidene fluoride suspensions

Solef® PVDF aqueous suspensions (XPH-859 and XPH-884) were used to develop highly stable EC electrodes, which were started to be produced by the Belgian company Solvay. Within the framework of the joint international project of the EU Energy Caps, we were tasked to investigate the possibilities of using these binders to obtain EC electrodes.

Aqueous suspensions contained amorphous polymers with a molecular weight of about 90,000; they are elastic in the solid state and have a globular structure (**Fig. 3.34**).

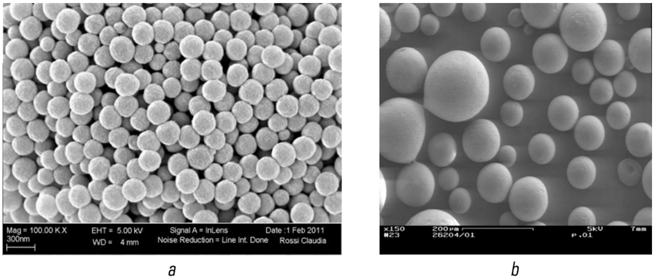

a *b*

Fig. 3.34 Scanning electron microscopy of the Solef KhRN-884 structure with different magnifications of PVDF particles: *a* – 300 nm/cm; *b* – 100 nm/cm

The concentration of Solef XPH-884 is 22 %, and Solef XPH-859 is 27 %. The polymers have different sedimentation resistance, which is low in Solef PVDF XPH-859. After some time, about 6 months, the Solef XPH-859 polymer precipitates and polymerizes to form an insoluble precipitate.

In addition, the surfactant in the Solef XPH-884 suspension has a pronounced foaming ability. Films obtained from these suspensions differ significantly in structure and their physical and mechanical properties (**Fig. 3.35**).

Thus, homogeneous, transparent, elastic films are formed from the Solef XPH-859 suspension, while films from Solef XPH-884 retain a clear globular structure, are quite fragile and opaque.

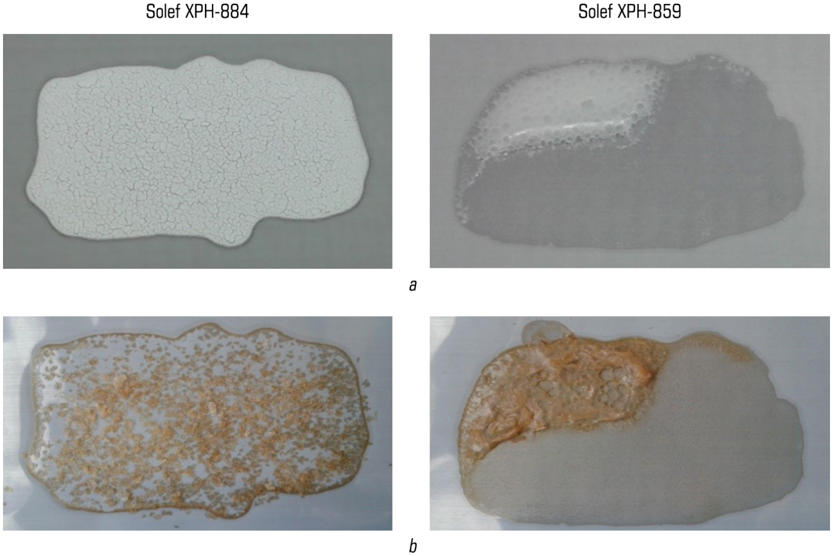

Fig. 3.35 Film structure after drying: *a* – at room temperature; *b* – at a temperature of 150 °C

The polymers feature stabilizing surface agents (Solef XPH-859 suspensions have a pH of approximately 4.5 and Solef XPH-884 ≈2.5), and Solvay limits information on polymer composition for confidentiality reasons. The joint between these suspensions is very low viscosity. This makes it impossible to produce a stable suspension for applying the active material to the current collector of the electrode. To increase the viscosity of the suspension, we proposed the use of NaCMC.

This polymer belongs to the rigid-chain ones, due to which it forms a slightly deformed structure. The rigidity of NaCMC macromolecules and the presence of active groups in them have a significant effect on the physical and mechanical properties of the active material of EC, the components of which are activated carbon and a conductive additive. On the particles of these components there are always active centers in the form of oxygen-containing groups, edges and corners of crystallites, other atoms. Naturally, their number depends on different methods of obtaining these materials and affects the formation of conductive structures in the composite. When preparing the mixture, it should be taken into account that the maximum viscosity of the NaCMC solution is achieved at a pH of about 7–9, and the used aqueous PVDF suspensions are acidic, which helps to reduce the viscosity of the working binder solution. The results showed that the use of these suspensions in combination with NaCMC has rather high electrochemical parameters compared to the classical PVDF polymer soluble in N-MP (**Table 3.16**) [47, 48].

● **Table 3.16** Internal resistance of EC* with electrodes made with different polymers

Polymer binders	**R_{ESR}, Ohm**	**R_{EDR}, Ohm**
Solef 6020 (from N-MP solution)	0.71	1.15
NaCMC/SBR (ratio 1/2)	1.10	2.70
NaCMC/XPH 859 (ratio 1/2)	0.37	1.43
NaCMC/XPH 884 (ratio 1/2)	0.44	1.15

**EC was assembled on the basis of Norit Supra 50 activated carbon and -1.5 M TEABF4 electrolyte in acetonitrile. The polymer content in the electrode was 10 %*

As for the adhesion strength of electrodes made using water-based polymer suspensions, it is higher than that of electrodes made using the standard method based on solutions of PVDF in N-MP (**Table 3.17**).

● **Table 3.17** The value of the internal resistance of EC based on electrodes made of various polymeric binders

Polymer binders	**P, N/m^2**	**Score at ASTM D 3359**
NaCMC/XPH 859 (ratio 1/2)	2420	3B
NaCMC /XPH 884 (ratio 1/2)	2519	3B
Solef PVDF 6020 (from N-MP solution)	2201	2B

Thus, the replacement of N-MP-based technology with a mixture of suspension PVDF and water-soluble NaCMC makes it possible to simplify the technology for manufacturing EC electrodes and obtain better results (by 38 %) in reducing the internal resistance of EC.

3.5 MANUFACTURING AND TESTING OF MODELS OF AN ELECTROCHEMICAL CAPACITOR

Selection of activated carbon for the production of EC electrodes

Carbon materials are widely used in various branches of technology and are used as adsorbents, carriers for catalysts, and catalysts themselves [49–55]. They are most widely used in adsorption processes. There are many different activated carbon materials that differ in origin and method of activation, for example, according to [56], more than 150 types of activated carbon (AC) are presented. The entire range of presented materials is characterized by narrowly specific areas of application, and so far the specific area of application of each new material is selected only empirically, and there is no single approach to predict the properties and behavior of AB in specific systems.

For example, it is known [56] that activated carbon selectively absorbs hydrocarbons and their derivatives, aromatic compounds, dyes, and, to a lesser extent, lower alcohols, carboxylic acids, and esters, and the chemical structure of the surface of the carbon material has a great influence on water adsorption [57]. For example, water adsorption does not occur on an unoxidized carbonaceous surface, and when the surface is oxidized, significant H_2O adsorption is noted, which can be increased by introducing alkaline earth metal ions and increases by a factor of 4–5 for alkali metal ions. Functional groups can be aliphatic radicals, hydrogen atoms, and various oxygen-containing compounds (hydroxyl, carboxyl, carbonyl, lactone, quinoid, etc.).

Each of the functional groups is attached to one carbon atom, the lactone group is already closed on two adjacent carbon atoms, and the quinoid group changes the electronic structure of the carbon atom associated with it.

The presence of such features leads to many options for implementing surface properties for the same initial structure [58]. Depending on the direction and method of surface transformation, various functional groups are formed and, accordingly, the surface can acquire directed specificity upon adsorption of certain molecules [59].

Since the capacitance of an electrochemical capacitor directly depends on the available surface area of the carbon material on which a double electric layer is formed, part of the work was focused on the selection of carbon material [60–63]. Samples of activated carbon brand Norit DLC (Netherlands) and YP-50F Kuraray Chemical Co (Japan) were selected for research [64]. The main characteristics of the samples are given in **Table 3.18**.

As can be seen from **Table 3.18**, activated carbon of the Supra 30 and Supra 50 brand has the largest surface area and micropore volume.

The EC characteristics are greatly affected by the pore size distribution. Supra 30 and Supra 50 activated carbons have very small pores, which are not available for $TEABF_4$ electrolyte.

The electrodes made from these samples of activated carbon were of poor quality. Due to the sufficiently high internal stress, the active layer of the electrode cracked and was characterized by low adhesion to the current collector. **Fig. 3.36** shows ASTM D 3359 test results for Supra 30 and Supra 50 activated carbon electrodes.

The active layer is completely detached when the adhesive tape is peeled off from the Kawatake Electrics Co. Grass Aluminum Foil.

Fig. 3.37 shows the results of the ASTM D 3359 test for the YP-50F activated carbon electrode.

Activated carbon of the YP-50F brand differed from previous brands in that the active layer has good adhesion to the metal current collector (**Fig. 3.37**) even with a lower content of polymer binder (6 % versus 10 %). High adhesion has a positive effect on the electrical characteristics of the electrode. It was found that EC based on YP-50F has a significantly lower internal resistance compared to EC based on Supra 50 activated carbon (**Table 3.19**). According to **Table 3.19** Internal resistance of Supra 50 based EC is 63 % higher than that of YP-50F activated carbon based EC.

Table 3.18 General characteristics of various types of activated carbon

General indicator	**Brands of activated carbon**				
	Super 30	**Supra 30**	**Super 50**	**Supra 50**	**YP-50F**
Total surface area (BET), m^2/h	1850	2100	1850	2100	1660
Imaginary density, kg/m^3	350	275	400	325	370
Micropore volume, cm^3/g	0.68	0.85	0.68	0.85	0.74
Mesopore volume, cm^3/h	0.07	0.1	0.07	0.1	0.21
Particle size D10, µm	2–4	2–4	3–5	3–5	5–20
Particle size D50, µm	5–10	5–10	9–13	9–13	
Particle size D90, µm	13–20	13–20	21–31	21–31	
Particle size D100, µm	30	30	50	50	
Ash content, %	2	2	2	2	0.3
Solvent components of ash, %	0.02	0.02	0.02	0.02	–
Chlorides, g/100g	0.04	0.04	0.04	0.04	–
Iron, ppm	40	40	40	40	–

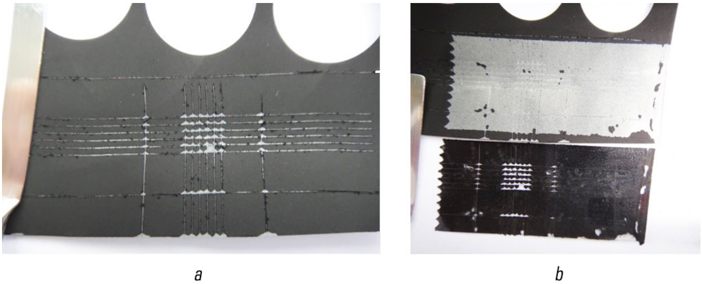

a

b

Fig. 3.36 Image of the electrode surface: *a* – after cutting; *b* – after peeling off the adhesive tape. Electrode composition: Supra 50 – 85 %, conductive additive – 5 %, polymer binder Solef-6020 – 10 %

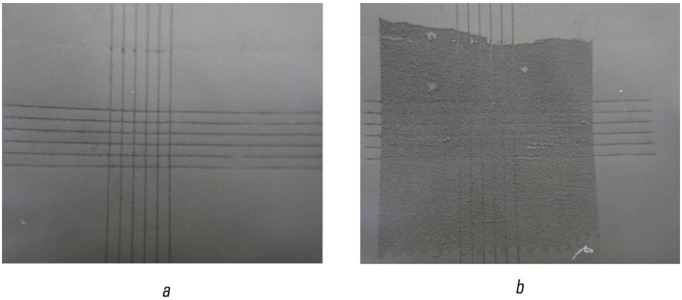

Fig. 3.37 Image of the electrode surface: *a* – after cutting; *b* – and peeling off the adhesive tape. Electrode composition: YP-50F – 89 %, conductive additive – 5 %, polymer binder Solef-6020 – 6 %

Table 3.19 EC internal resistance based on different brands of activated carbon

Activated carbon	**R_{ESR}, Ohm**	**R_{EDR}, Ohm**
Supra 50	1.2	3.9
YP-50F	0.89	1.43

In order to establish the reasons for the different characteristics of electrodes based on activated carbon samples with fairly similar physical and chemical characteristics (**Table 3.18**), microscopic studies of the structure of the samples were carried out. Activated carbon Norit Supra 50 after soft dispersion has a fine structure (**Fig. 3.38, *a***) with a small amount of soot chains, unlike YP-50F carbon (**Fig. 3.38, *b***).

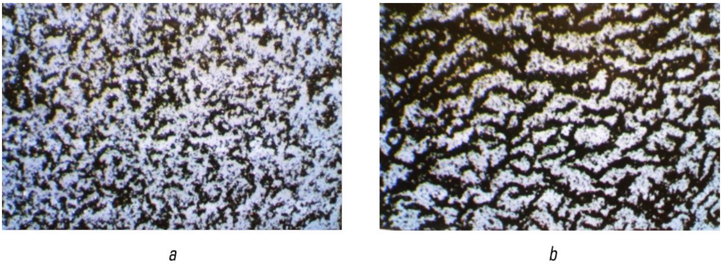

Fig. 3.38 Microstructure of activated carbon film: *a* – Norit Supra 50; *b* – YP-50F at 7x magnification

Thus, the YP-50F activated carbon covers the metal foil more compactly. This is due to the secondary structure of the particles of said sample of activated carbon. **Fig. 3.39** shows the results of electron microscopic studies of YP-50F coal.

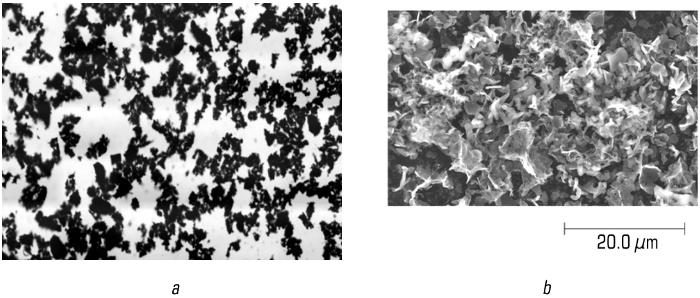

Fig. 3.39 Microstructure of activated carbon particles: *a* – YP-50F magnification; *b* – magnification by 200 times

From **Fig. 3.39** it follows that activated carbon particles up to 20 μm form a secondary structure in the form of compact chains. It is possible that such a structure makes it possible to obtain a compact coating on the current collector.

The structure formation of finely dispersed carbon materials can be assessed by oil absorption. To this end, the oil absorption of various carbon materials was established. The results of the study are given in **Table 3.20**.

Table 3.20 Oil absorption value of different carbon materials

Carbon material	**Oil absorption, ml/g**
Norit Supra 50	1.6
Norit Super 50	1.9
Norit Supra 30	1.7
Norit Super 30	1.8
YP-50F	2.2
Graphite soot (Pure Black-205)	3.8
Graphite carbon soot (Super C65)	9.4
Acetylene soot	2.8
Acetylene soot (Shawinigan)	7.9

Selection of conductive additive

The specific characteristics of the activated carbon particles and the conductive additive can affect their interaction with the polymer macromolecules. Such characteristics can be considered the chemical nature, size, shape, granulometric composition, specific surface area (geometric, total), real and bulk density, porosity, particle packing, surface pH.

The hydrogen index of the water extract from carbon materials makes it possible to speak about their wetting, selective adsorption, and the ability to aggregate particles.

Nevertheless, the nature of surface active centers has the main influence on the intermolecular interactions of the polymer-filler and filler-filler [65]. Such active centers on carbon particles can be unpaired electrons, foreign atoms and groups of atoms (primarily oxygen), and crystallite lattice defects. In turn, the nature and number of active centers depend on the technology for obtaining carbon particles.

The primary structure of carbon black (soot) is chaotically arranged packets of planar molecular layers [66]. These fine layers have a structure similar to graphite, but are irregularly arranged. Such crystallites are linked by valence bonds and form two- or three-dimensional racemose aggregates. Considering all this, one of the important components of electrode masses is a conductive additive, which provides reliable contact between the system components and promotes better wetting with electrolyte [67–70]. Among these additives, we chose Super C65 carbon black with a density of 160 kg/m^3, which differed from others in its good dispersion and ensured reliable contact between active material lobules [71].

Fig. 3.40 shows a schematic model of the arrangement of particles of a carbonaceous conductive additive in an EC electrode. Using this model, it is possible to explain how exactly the conductive additive works and according to what scheme the charge is transferred to the current collector [72].

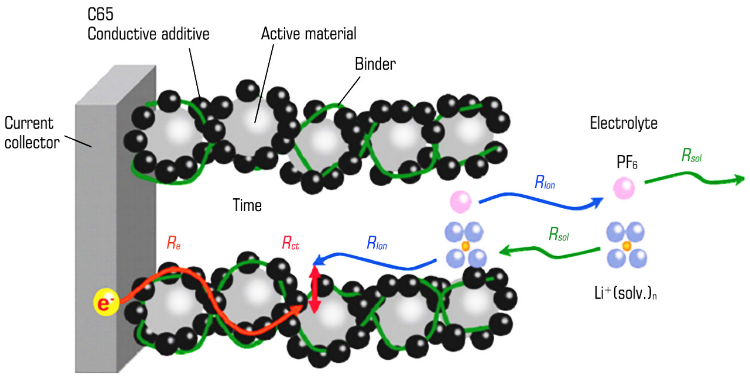

Fig. 3.40 Schematic representation of the location of the particles of the conductive additive C65

As can be seen from **Table 3.20**, graphitized carbon black Super C65 demonstrates maximum oil absorption, which is characterized by a good structure formation factor and, accordingly, the ability to form chains of soot lobules for reliable electrical contact of all components (**Fig. 3.41**).

The ability to structure increases with an increase in the degree of dispersion of particles and a decrease in the amount of volatile impurities in them.

The specificity of the electrode mass is that it should have maximum electrical conductivity with a minimum amount of polymer binder, which ensures the mechanical strength of the electrode. It is known that a small content of a solid dispersed filler in a polymer can increase the strength of the composite, since cracks growing under the action of a load are stopped by filler particles. However, an excessive concentration of filler increases the brittleness of the material.

In our case, the maximum oil absorption provides the greatest value of structure formation on the one hand, but also has the greatest shrinkage after drying on the other (**Fig. 3.42**).

The samples were prepared in the ratio of carbon material – 90 %, polymer binder (sodium salt of carboxymethyl cellulose) – 10 %. As can be seen from **Fig. 3.42**, the greatest shrinkage was observed precisely in Super C65, which had the maximum oil absorption value of all carbon materials, which indicates a fairly strong intermolecular interaction between carbon segments. In addition, Super C65 is sufficiently well dispersed and wetted by electrolyte, which has a positive effect on the electrochemical characteristics of EC.

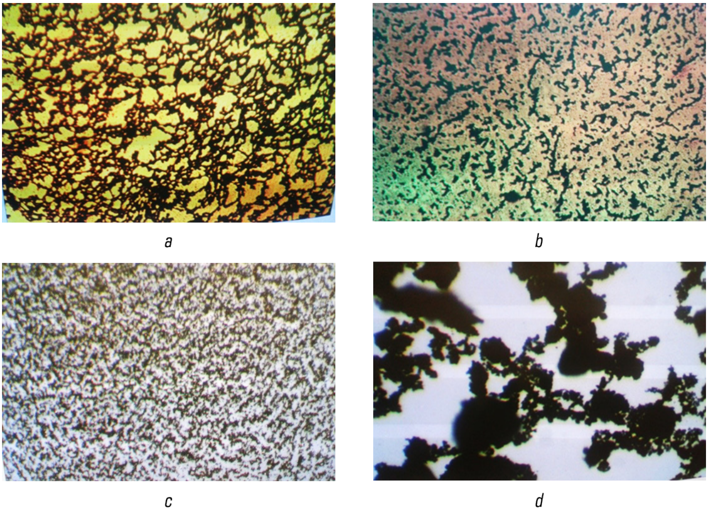

Fig. 3.41 Micrographs of structures of various electrically conductive materials at 7x magnification: *a* – Super C65; *b* – acetylene soot; *c* – acetylene soot (Shawinigan); *d* – graphitized carbon soot (PureBlack-205)

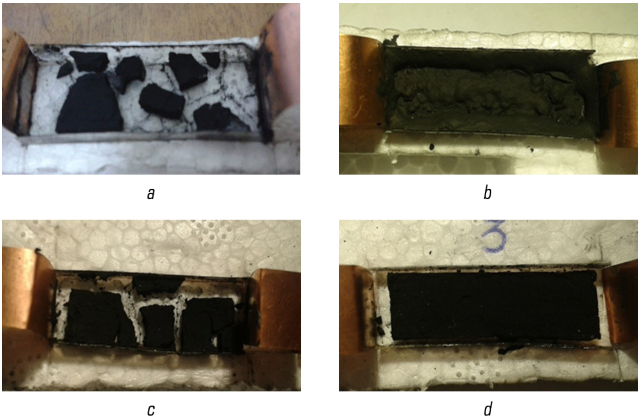

Fig. 3.42 Image of shrinkage of a composite material based on various types of conductive additives after drying of the polymer binder: *a* – Super C65; *b* – acetylene soot; *c* – carbon Black 001; *d* – Pure Black

Optimization of the composition of the EC electrode

As was shown earlier, the state of the surface of the current collector of the electrode has a significant effect on the adhesion of the polymer [73, 74]. Therefore, surface-modified aluminum foil from Kawatake Electronics Co. was preferred as the metal current collector (Japan). As shown in **Fig. 3.43**, the contact surface of the active material and the metal is significantly increased due to the high porosity of the surface layer of the foil. Therefore, the production of EC electrodes was realized on the basis of aluminum foil from Kawatake Electronics Co. (Japan).

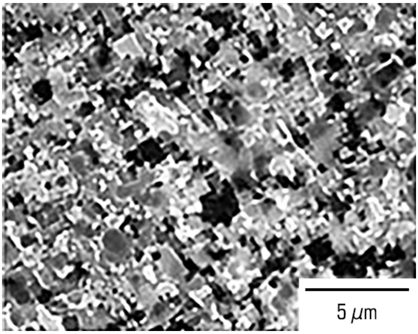

Fig. 3.43 Surface microstructure of modified aluminum foil

In this work, nitrogen sorption isotherms were obtained for electrode material samples based on selected YP-50F activated carbon and various polymeric materials. **Fig. 3.44** shows isotherms of sorption and desorption of nitrogen.

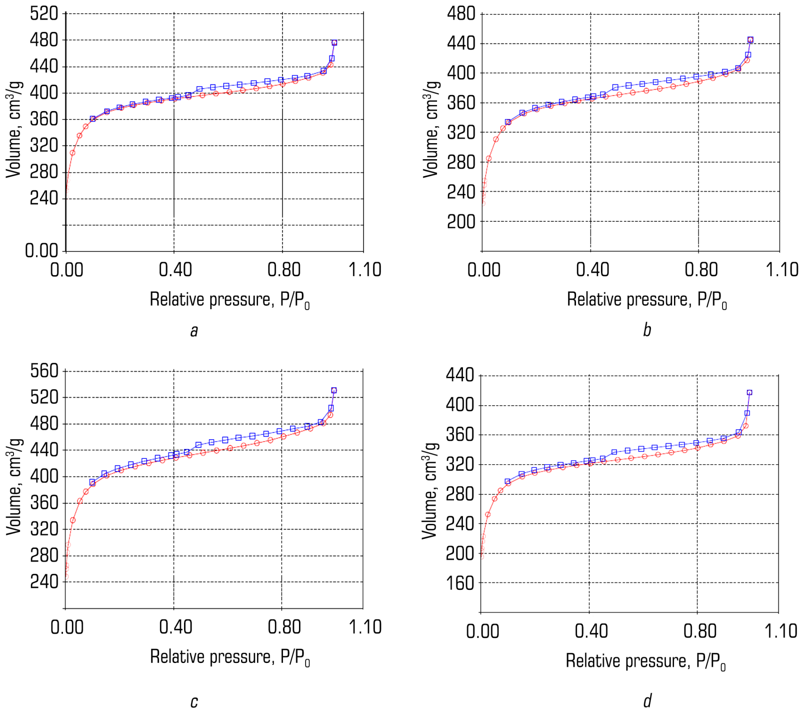

a *b*

c *d*

Fig. 3.44 Adsorption – desorption isotherms of an electrode composite based on YP-50F activated carbon and various polymeric materials:
a – SBR; *b* – Solef XPH-859; *c* – Solef XPH-884; *d* – Solef 6020

The obtained isotherms are typical for polymolecular adsorption in micro and mesopores of cellular materials. For all samples, the isotherms show a hysteresis loop, which is associated with capillary condensation in mesopores. The parameters of the porous structure of the electrode compositions were determined based on the analysis of nitrogen adsorption/desorption isotherms.

As can be seen from **Fig. 3.45** and **3.46**, the introduction of a polymeric binder leads to a decrease in the specific surface area and total pore volume of the electrode composite.

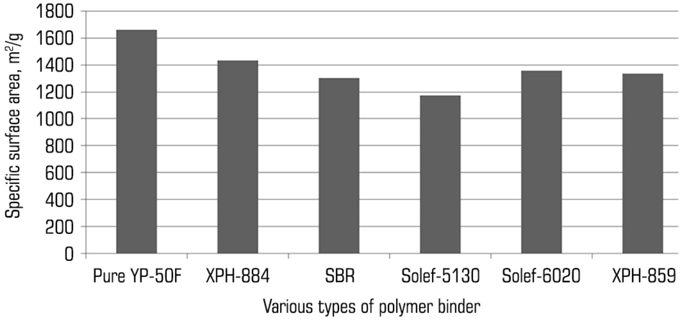

Fig. 3.45 Specific surface of the electrode composite based on YP-50F activated carbon and various polymeric materials (dry binder content – 10 %)

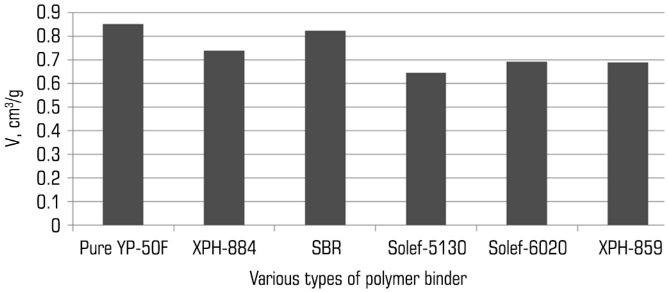

Fig. 3.46 Total pore volume of the electrode composite based on YP-50F activated carbon and various polymeric materials (10 % of the binder by dry residue)

According to the results of the study, the use of an aqueous suspension of Solef XPH-884 and SBR as a polymer for the electrode mass, in combination with a soluble sodium salt of CMC, makes it possible to obtain composites with the maximum specific surface area and the largest total pore volume. It should be noted that this binder fully met all the requirements for a polymer binder in the manufacture of electrochemical current sources [75–77]. The electrode composite had good adhesion to the metal current collector, ensured reliable connection of all components of the system, and left the surface of the active material as accessible as possible, which was confirmed by analysis.

Considering all the results obtained, a combination of an aqueous suspension of Solef XPH-884 with NaCMC in a ratio of 2:1 was proposed as a binder polymer. The latter served as a polymeric thickener and provided the necessary viscosity of the suspension for applying it to the metal current collector by the doctor blade method (**Fig. 3.47**).

The first step in the manufacture of electrodes was to obtain a working solution of polymers containing a dispersed electrically conductive additive. To do this, a weighed portion of the Super C65 conductive additive was added to a solution of Solef XPH-884 with NaCMC in a ratio of 2:1 in three stages. Each introduction of carbon material into the solution was accompanied by mechanical stirring for 15 min and 10 min. The electrode mass was subjected to the action of ultrasound. Activated carbon YP-50F was also added to the prepared solution in three stages. To achieve a homogeneous mass, a combination of mechanical mixing and ultrasonic dispersion was also carried out. The second stage was the direct application of the electrode mass to the current collector. After the final drying, the electrodes were compacted by rolling at a temperature of 100 °C.

The microstructure of the obtained electrode is shown in **Fig. 3.48**.

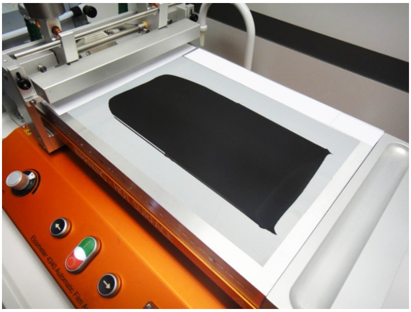

Fig. 3.47 Image of the electrode on the device Dr. Blade after applying the YP-50F activated carbon suspension and the combination of Solef XPH-884 aqueous emulsion with NaCMC in a ratio of 2:1

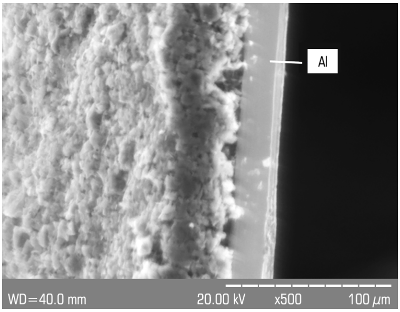

Fig. 3.48 Photomicrograph of the surface and side cut of an electrode based on activated carbon YP-50F and a combination of an aqueous suspension of Solef XPH-884 with NaCMC in a ratio of 2:1

The active material layer has high strength and adheres tightly to the metal current collector. Also, the conductive additive is evenly distributed in the active layer. According to **Fig. 3.48**, the correct selection of technological parameters for applying an electrode suspension makes it possible to avoid the well-known defects of the electrode layer, which are typical for the manufacture of electrodes based on aqueous suspensions of polymers. In particular, there are no formations of agglomerates and holes in the electrode layer of the electrode.

Electrical characteristics of EC laboratory prototypes

In this work, compact ECs with an organic electrolyte were fabricated. EC mock-ups were made using body parts of primary lithium CDM of CR2016 size (**Fig. 3.49**).

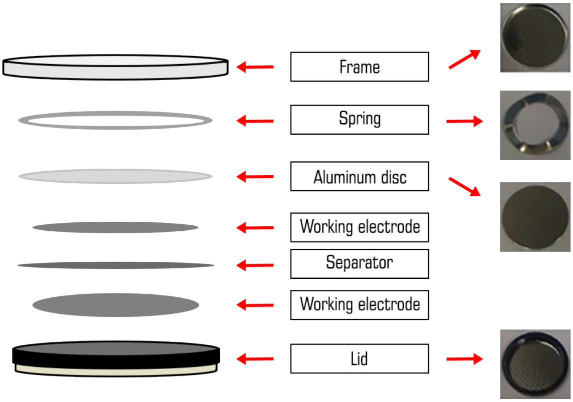

Fig. 3.49 Structural components of EC size CR2016

Various organic electrolytes have been studied in this work. A solution of $TEABF_4$ in acetonitrile has the best electrical conductivity. For example, 1.5 M $TEABF_4$ in acetonitrile has the highest electrical conductivity (over 60 mS/cm) of organic electrolytes and allows the operation of electrochemical systems down to –40 °C.

However, such solutions have high chemical activity with respect to stainless steel-based EC body parts. Corrosion of body parts complicates the development of the EC design based on them. An aluminum disk 0.5 mm thick is used to protect the body parts. The electrolytes of lithium current sources allow the use of stainless steel body parts, which simplifies the selection and design of the EC, but they are significantly lower in electrical conductivity (13–15 mS/cm).

In the work, models of electrochemical capacitors based on manufactured electrodes with different electrolytes were compiled and tested. The CVs of capacitors with electrodes based on various electrolytes are shown in **Fig. 3.50**. The curves are rectangular, which is typical for an ideal capacitor. On the CV of a capacitor with an electrolyte composition of 1.2 M LiTFSI in acetonitrile, a sharp increase in current is observed at a voltage above 2.5 V.

This may indicate the passage of corrosion processes in such EC.

Fig. 3.51 shows the impedance spectra of a symmetrical capacitor based on different electrolytes.

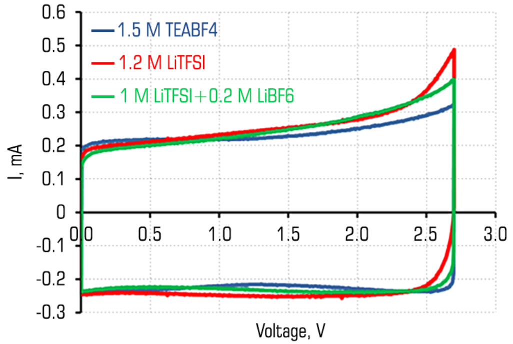

⬡ **Fig. 3.50** CVA EC based on different electrolytes; EC voltage sweep rate – 10 mV/s

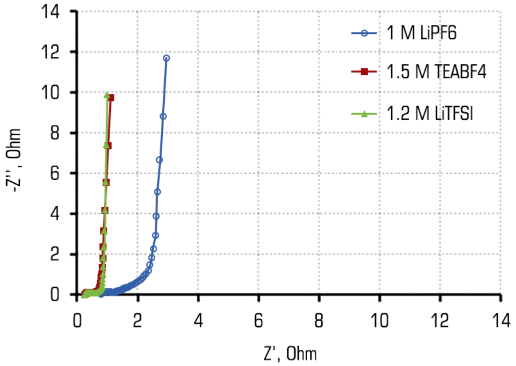

⬡ **Fig. 3.51** Nyquist dependence of EC based on various electrolytes

The internal resistance of capacitors made with lithium battery electrolytes (1M $LiPF_6$ in EC:DMC) is three times higher than EC.

Therefore, we fabricated and studied ECs based on YP-50F activated carbon with the proposed combined composite binder: NaCMC Solef XPH-884 and electrolyte 1.5 M $TEABF_4$ in acetonitrile.

For comparison, ECs were also studied with electrodes made from binding PVDF according to the standard method (using solutions of PVDF in N-MP). The electrical characteristics of the developed EC are given in **Table 3.21**.

Table 3.21 Specific characteristics of laboratory models of EC

Electrode material		**Characteristics***			
Activated carbon	**Bonding material**	**Voltage, V**	**W, W·h/kg**	**Resistance, Ohm·cm**	**Pмax, kW/kg**
YP-50F	Solef-6020	3.0	29	0.88	47
YP-50F	Solef-5130	3.0	26	1.43	34
YP-50F	Solef XPH-884 with NaCMC	3.0	33	0.67	73

* *electrical characteristics are calculated without taking into account the mass of the EC body*

In terms of electrical characteristics, the ECs based on a mixture of suspension PVDF and water-soluble NaCMC are not inferior to analogs manufactured by the standard method. One of the main advantages of the developed ECs is the avoidance of using the toxic organic solvent N-MP [78, 79]. This made it possible to ensure a low cost of EC production and improve the environmental situation in the manufacture of EC electrodes.

Laboratory studies of EC based on the proposed electrode composite showed that there is no significant change in their electrical characteristics after cycling. Experimental data obtained during the first 100 cycles show that the total capacitance loss of the capacitor is 3 %. The drop in capacity after a cycle for 10,000 charge/discharge cycles was less than 5 %.

CONCLUSIONS

1. A technology has been developed for producing electrodes based on a mixture of an aqueous suspension of PVDF (Solef XPH-884) and a water-soluble sodium salt of CMC. These electrodes are not inferior in electrochemical characteristics to electrodes made using PVDF solutions, and in some cases even surpass them (for example, they provide a decrease in internal resistance up to 40 %). Due to the use of water-based components, the production of EC becomes cheaper and more environmentally friendly.

2. Taking into account the results of a comparative analysis of a series of PVDF samples of various modifications synthesized by Solvay, PVDF-6020 homopolymer and PVDF-5130 copolymer brands were chosen as a binder in electrode compositions. Of these, PVDF-5130 has the best adhesive properties (by 40÷75 %). However, this polymer significantly blocks the surface of activated carbon, thereby doubling the internal resistance of the EC, so its concentration in the electrode should not exceed 4 %.

3. The possibility of replacing the N-MP solvent for the PVDF polymer with a safer DMSO solvent for the manufacture of EC electrodes has been proven. The technological process of applying a suspension of the active material based on DMSO should be carried out at a temperature of 40–60 °C. The presence of functional groups in the polymer (for example, as in PVDF Solef-5130) leads to an increase in the content of sulfur-containing products (up to 400–600 g) in the active layer of the electrode. The source of sulfur-containing compounds are the decomposition products of DMSO. Getting into the electrolyte EC, they cause side reactions leading to self-discharge of the EC and limiting its operating voltage to 1.5 V, as well as a drop in capacity during cycling. However, the replacement of the toxic solvent by DMSO becomes possible with additional washing of the EC electrodes with ethyl alcohol.

4. Comprehensive studies have been carried out on the process of formation of EC strip electrodes with an active layer thickness of up to 100 μm. Technological parameters of the process of formation of EC electrodes and their operational characteristics are established. A technological scheme for the production of electrodes is proposed.

5. It is shown that the highest capacity of electrodes based on an aqueous suspension of PVDF and water-soluble NaCMC corresponds to a polymer content of 6 %; drying of the electrodes should be carried out in two stages – at 60 °C for 15...20 minutes, then at 120 °C in a vacuum; the density of the active layer of electrodes should be 0.6...0.8 g/cm^3; Increasing the temperature of the rollers during rolling up to 100 °C makes it possible to increase the density and strength of the electrodes up to 2 times.

6. Prototypes of stable ECs have been developed, where for the first time new composite materials based on a mixture of water-soluble suspensions of PVDF (Solef XPH-884) and NaCMC are used. The specific energy of laboratory prototypes of ECs is 33 Wh/kg, which is almost an order of magnitude higher than the energy of traditional ECs with electrodes made using PVDF solutions in N-MP.

CONFLICT OF INTEREST

The authors declare that they have no conflict of interest in relation to this research, whether financial, personal, authorship or otherwise, that could affect the research and its results presented in this paper.

REFERENCES

1. Wang, Y., Song, Y., Xia, Y. (2016). Electrochemical capacitors: mechanism, materials, systems, characterization and applications. Chemical Society Reviews, 45 (21), 5925–5950. doi: https://doi.org/10.1039/c5cs00580a

2. Ali, A., Andriyana, A. (2020). Properties of multifunctional composite materials based on nanomaterials: a review. RSC Advances, 10 (28), 16390–16403. doi: https://doi.org/10.1039/c9ra10594h
3. Malietin, Yu., Stryzhakova, N., Zelinskyi, S. et al. (2011). Cuperkondensatory – nakopychuvachi elektrychnoi enerhii z vykorystanniam nanorozmirnykh vuhletsevykh materialiv. Visnyk NAN Ukrainy, 12, 23–29.
4. Vivekchand, S. R. C., Rout, C. S., Subrahmanyam, K. S., Govindaraj, A., Rao, C. N. R. (2008). Graphene-based electrochemical supercapacitors. Journal of Chemical Sciences, 120 (1), 9–13. doi: https://doi.org/10.1007/s12039-008-0002-7
5. Stoller, M., Zhu, Y., Ruoff, R. (2008). Graphene-based ultracapacitors. Proc. 18th Intern. Seminar on Double Layer Capacitors and Hybrid Energy Storage Devices, 4–7.
6. Burke, A. (2007). R&D considerations for the performance and application of electrochemical capacitors. Electrochimica Acta, 53 (3), 1083–1091. doi: https://doi.org/10.1016/j.electacta.2007.01.011
7. Kurzweil, P. (2009). HISTORY | Electrochemical Capacitors. Encyclopedia of Electrochemical Power Sources, 596–606. doi: https://doi.org/10.1016/b978-044452745-5.00006-x
8. Noori, A., El-Kady, M. F., Rahmanifar, M. S., Kaner, R. B., Mousavi, M. F. (2019). Towards establishing standard performance metrics for batteries, supercapacitors and beyond. Chemical Society Reviews, 48 (5), 1272–1341. doi: https://doi.org/10.1039/c8cs00581h
9. Murphy, T. C., Wright, R. B., Sutula, R. A. (1997). Electrochemical Capacitors II, Proceedings. The Electrochemical Society. Pennington, 96, 258.
10. Miller, J. R., Burke, A. (2008). Electrochemical Capacitors: Challenges and Opportunities for Real-World Applications. The Electrochemical Society Interface, 17 (1), 53–57. doi: https://doi.org/10.1149/2.f08081if
11. Delhaes, P. (2019). Graphite and Precursors. CRC Press, 312.
12. Drobnyi, D. M., Tychyna, S. O., Stryzhakova, N. H., Malietin, Yu. A. (2015). Polimerni materialy dlia kompozytnykh elektrodiv superkondensatoriv. Perspektyvni polimerni materialy ta tekhnolohii. Kyiv, 19–23.
13. Malietin, Yu. A., Shembel, O. M., Novak, P., Podmohilnyi, S. M., Stryzhakova, N. H., Izotov, V. Yu. et al. (2010). Pat. Ukrainy No. 90448 UA. Metod vyhotovlennia elektrodiv z nyzkym kontaktnym oporom dlia batarei ta kondensatoriv podviinoho sharu. MPK: H01G 9/00, H01G 9/155 (2006.01). No. a200506296. declareted: 25.06.2005; published: 11.15.2010.
14. Izotov, V. Yu., Biriukova, Yu. V. (2008). Pat. No. 35069U. Elektrod dlia kondensatoriv podviinoho elektrychnoho sharu. MPK: H01G 9/00. No. u200805440. declareted: 25.04.2008; published: 26.08.2008.
15. Baklan, V. Yu., Korolenko, S. D. (2010). Stan ta perspektyvy rozvytku khimichnykh dzherel strumu. Visnyk KNUTD, 5, 227–232.
16. Merena, R. I., Budzuliak, I. M., Hryhorchak, I. I. et al. (2004). Doslidzhennia kharakterystyk elektrokhimichnykh kondensatoriv, sformovanykh na osnovi aktyvovanoho vuhletsiu, modyfikovanoho vysokotemperaturnoiu obrobkoiu. Fizyka i khimiia tverdoho tila, 5 (4), 836–839.

17. Béguin, F., Presser, V., Balducci, A., Frackowiak, E. (2014). Carbons and Electrolytes for Advanced Supercapacitors. Advanced Materials, 26 (14), 2219–2251. doi: https://doi.org/10.1002/adma.201304137
18. Conway, B. E. (1999). Electrochemical supercapacitors. Scientific fundamentals and technological applications. New York, 698.
19. Drobnyi, D. (2017). Pat. No. WO2017025792 A1. Sposob izgotovleniia elektroda dlia elektrokhimicheskogo kondensatora dvoinogo sloia. MPK: H01G11/86; declareted: 09.08.2016; published: 16.02.2017.
20. Pashkevich, K., Yezhova, O., Kolosnichenko, M., Ostapenko, N., Kolosnichenko, E. (2018). Designing of the complex forms of women's clothing, considering the former properties of the materials. Man-Made Textiles in India, 46 (11), 372–380.
21. Ellis, B., Smith, R. (2020). Polymers A Property Database. CRC Press, 1052.
22. Horonovskyi, Y. T., Nazarenko, Yu. P., Nekreh, E. F. (1974). Kratkyi spravochnyk po khymyy. Kyiv: Naukova dumka, 830.
23. Barzic, A. I., Rawat, N. K., Haghi, A. K. (Eds.) (2021). Imidic Polymers and Green Polymer Chemistry. New York: Apple Academic Press, 380. doi: https://doi.org/10.1201/9781003057918
24. Schwartz, M. (2008). Smart Materials. CRC Press, 554.
25. Marphy, R., Krehl, P., Liang, C. (1981). Technologies for the Transition. 16th Intersociety Energy Conversion Engineering Conference. New York, 1, 97.
26. Perelmuter, V. (2017). Electrotechnical Systems. Simulation with Simulink® and SimPowerSystems™. CRC Press, 450.
27. Gür, T. M. (2018). Review of electrical energy storage technologies, materials and systems: challenges and prospects for large-scale grid storage. Energy & Environmental Science, 11 (10), 2696–2767. doi: https://doi.org/10.1039/c8ee01419a
28. Broussely, M., Bodet, J. M., Staniewicz, R. J. (1994). Proceedings of the Symposium on Rechargeable Lithium and Litium-ion Batteries. Extended Abstracts of Fall Meeting of the Electrochemical Society. Maimi Beach, 224.
29. Pat. No. 2249455 FR. Kondensator pereminnoi yemnosti (1975). Kl. N01 m 13/06, declareted: 29.10.73, published: 23.05.75.
30. Haghi, A. K., Ribeiro, A. C. F., Pogliani, L., Balköse, D., Torrens, F., Mukbaniani, O. V. (2021). Applied Chemistry and Chemical Engineering, Research Methodologies in Modern Chemistry and Applied Science. Apple Academic Press, 390.
31. Moore, J. H., Spencer, N. D. (2001). Encyclopedia of Chemical Physics and Physical Chemistry. CRC Press, 2814.
32. Uendland, U. (1978). Termicheskie metody analiza. Moscow, 279.
33. Song, M.-K., Cairns, E. J., Zhang, Y. (2013). Lithium/sulfur batteries with high specific energy: old challenges and new opportunities. Nanoscale, 5 (6), 2186–2204. doi: https://doi.org/10.1039/c2nr33044j

34. Kolosnichenko, O., Yakovlev, M., Prykhodko-Kononenko, I., Tretyakova, L., Ostapenko, N., Pashkevich, K., Ripka, G. (2020). Study of dominant quality indicators of materials and designs of railroad conductors' uniforms. Vlákna a textile, 3 (27), 90–96.
35. Shlaiker, C., Young, C. (1980). Batteries for implantable biomedical devices. 29th Power Sources Symposium, 129.
36. Borshch, A. V., Chernysh, O. V. (2016). Porivniannia kharakterystyk polivinilidenftorydiv 6020 ta 5130 v elektrodnykh kompozytnykh materialakh. Naukovi rozrobky molodi na suchasnomu etapi, 1, 297.
37. Zaiets, O. V., Tverdokhlib, V. S. (2004). Vlastyvosti polimernoho zv'iazuiuchoho aktyvnykh mas litii-ionnykh dzherel strumu. Naukovi rozrobky molodi na suchasnomu etapi, 1, 159.
38. Zaiets, O. V., Tverdokhlib, V. S. (2005). Vyvchennia vlastyvostei polimernoho zv'iazuiuchoho PVDF u yon-litiievykh dzherelakh strumu. Naukovi rozrobky molodi na suchasnomu etapi, 1, 184.
39. Chernysh, O. V., Khomenko, V. H., Barsukov, V. Z., Borshch, A. V. (2016). Vplyv tekhnolohichnykh modyfikatsii polivinilidenftorydu na fizyko-mekhanichni vlastyvosti elektrodiv khimichnykh dzherel strumu. Visnyk KNUTD, 5, 141–148.
40. Wang, F., Wu, X., Yuan, X., Liu, Z., Zhang, Y., Fu, L., Zhu, Y., Zhou, Q., Wu, Y., Huang, W. (2017). Latest advances in supercapacitors: from new electrode materials to novel device designs. Chemical Society Reviews, 46 (22), 6816–6854. doi: https://doi.org/10.1039/c7cs00205j
41. Zaiets, O. V., Kolodii, I. O., Mykoliuk, S. V. (2006). Optymizatsiia umov vysushuvannia aktyvnykh mas litii-ionnykh KhDS. Naukovi rozrobky molodi na suchasnomu etapi, 1, 232.
42. Veres, A. R., Drahan, D. R., Chernysh, O. V. (2014). Mozhlyvosti vykorystannia vodorozchynnykh zv'iazuiuchykh v kompozytnykh elektrodnykh materialakh. Naukovi rozrobky molodi na suchasnomu etapi, 1, 367–368.
43. Zhao, W. (2020). Handbook for Chemical Process Research and Development. CRC Press, 858.
44. Simon, P., Gogotsi, Y. (2020). Perspectives for electrochemical capacitors and related devices. Nature Materials, 19 (11), 1151–1163. doi: https://doi.org/10.1038/s41563-020-0747-z
45. Wypych, G. (2016). Handbook of Polymers. ChemTec Publishing, 706. doi: https://doi.org/10.1016/c2015-0-01462-9
46. Namsheer, K., Rout, C. S. (2021). Conducting polymers: a comprehensive review on recent advances in synthesis, properties and applications. RSC Advances, 11 (10), 5659–5697. doi: https://doi.org/10.1039/d0ra07800j
47. Barsukov, V. Z., Khomenko, V. G., Chernysh, O. V. et al. (2016). Perspektivnye materialy i tekhnologii dlia sovremennykh KhIT i elektronnoi tekhniki. Sovremennye elektrokhimicheskie tekhnologii i oborudovanie. Minsk, 147–148.
48. Barsukov, V., Khomenko, V., Chernysh, O., Makyeyeva, I. (2016). Modern materials for lithium-ion batteries and supercapacitors. 11th International conference on physics of advanced materials. Cluj-Napoca, 122.

49. Hank Ellison, D. (2022). Handbook of Chemical and Biological Warfare Agents. CRC Press, 838. doi: https://doi.org/10.4324/9781003230564
50. Saldívar-Guerra, E., Vivaldo-Lima, E. (Eds.) (2013). Handbook of Polymer Synthesis, Characterization, and Processing. John Wiley & Sons, Inc., 622. doi: https://doi.org/10.1002/9781118480793
51. Lendlein, A., Sisson, A. (Eds.) (2001). Handbook of Biodegradable Polymers: Synthesis, Characterization and Applications. WILEY-VCH, 426.
52. Balköse, D., Horak, D., Šoltés, L. (2021). Key Engineering Materials, Current State-of-the-Art on Novel Materials. Apple Academic Press, 584.
53. Roy Crompton, T. (2017). Organic Compounds in Natural Waters Analysis and Determination. CRC Press, 306.
54. Peebles, L. H. (1995). Carbon Fibers Formation, Structure, and Properties. CRC Press, 218.
55. Dragan, E. S. (2021). Advanced Separations by Specialized Sorbents. CRC Press, 358.
56. Webster, G. K., Kott, L. (Eds.) (2019). Chromatographic Methods Development. Jenny Stanford Publishing, 566. doi: https://doi.org/10.1201/9780429201721
57. Uwamariya, V. (2014). Adsorptive Removal of Heavy Metals from Groundwater by Iron Oxide Based Adsorbents. CRC Press, 160.
58. Barsukov, V. Z., Il'in, E. A., Likhnitskii, K. V., Zayats, O. V., Tverdokhleb, V. S., Kryukov, V. V. et al. (2008). Graphites from the Zavalie deposit as active materials for lithium-ion batteries. Russian Journal of Electrochemistry, 44 (5), 579–584. doi: https://doi.org/10.1134/s1023193508050121
59. Lynch, C. T. (2021). CRC Handbook of Materials Science. Material Composites and Refractory Materials. CRC Press, 654.
60. Barsukov, V. Z., Chernysh, O. V., Plavan, V. P. (2013). Stiikist do okyslennia zvychainoho i modyfikovanoho rozshyrenoho hrafitu. Tekhnolohii ta dyzain. Khimichni tekhnolohii ta ekolohichna bezpeka, 3, 1–8.
61. Khomenko, V. H., Barsukov, V. Z., Makieieva, I. S., Chernysh, O. V. (2016). Vplyv hrafitovykh materialiv na elektrychni kharakterystyky litii-ionnykh kondensatoriv. Perspektyvni materialy ta protsesy v tekhnichnii elektrokhimii. Kyiv, 22–26.
62. Zaiets, O. V., Shkromyda, R. V., Davydov, O. S. (2006). Vplyv dyspersnosti chastochok na vlastyvosti pryrodnoho hrafitu. Naukovi rozrobky molodi na suchasnomu etapi, 1, 233.
63. Barsukov, V., Langouche, F., Khomenko, V., Makyeyeva, I., Chernysh, O., Gauthy, F. (2015). Modeling of porous graphite electrodes of hybride electrochemical capacitors and lithium-ion batteries. Journal of Solid State Electrochemistry, 19 (9), 2723–2732. doi: https://doi.org/10.1007/s10008-015-2835-6
64. Kim, J.-A., Park, I.-S., Seo, J.-H., Lee, J.-J. (2014). A Development of High Power Activated Carbon Using the KOH Activation of Soft Carbon Series Cokes. Transactions on Electrical and Electronic Materials, 15 (2), 81–86. doi: https://doi.org/10.4313/teem.2014.15.2.81

65. Chernysh, S. I., Chernysh, I. H., Nikitin, Yu. O., Loboda, P. I. (2008). Pro vplyv metodiv dysperhuvannia na mikrostrukturu i morfolohiiu dyspersnykh chastynok pryrodnoho hrafitu ta termohrafenitu. Naukovi visti NTUU "KPI", 1, 76–80.
66. Wang, G., Yu, M., Feng, X. (2021). Carbon materials for ion-intercalation involved rechargeable battery technologies. Chemical Society Reviews, 50 (4), 2388–2443. doi: https://doi.org/10.1039/d0cs00187b
67. Struminska, T. V., Kolosnichenko, S. I., Chuprina, E. V., Ostapenko, N. V. (2019). Designing of special clothing based on experimental researches of material properties. Fibres and Textiles, 26 (4), 84–95.
68. Khomenko, V., Raymundo-Piñero, E., Béguin, F. (2008). High-energy density graphite/AC capacitor in organic electrolyte. Journal of Power Sources, 177 (2), 643–651. doi: https://doi.org/10.1016/j.jpowsour.2007.11.101
69. Cao, W. J., Zheng, J. P. (2012). Li-ion capacitors with carbon cathode and hard carbon/stabilized lithium metal powder anode electrodes. Journal of Power Sources, 213, 180–185. doi: https://doi.org/10.1016/j.jpowsour.2012.04.033
70. Schroeder, M., Winter, M., Passerini, S., Balducci, A. (2012). On the Use of Soft Carbon and Propylene Carbonate-Based Electrolytes in Lithium-Ion Capacitors. Journal of The Electrochemical Society, 159 (8), A1240–A1245. doi: https://doi.org/10.1149/2.050208jes
71. Rezqita, A., Hamid, R., Schwarz, S., Kronberger, H., Trifonova, A. (2015). Conductive Additive for Si/Mesoporous Carbon Anode for Li-Ion Batteries: Commercial Graphite vs Carbon Black C65. ECS Transactions, 66 (9), 17–27. doi: https://doi.org/10.1149/06609.0017ecst
72. Schütter, C., Ramirez-Castro, C., Oljaca, M., Passerini, S., Winter, M., Balducci, A. (2014). Activated Carbon, Carbon Blacks and Graphene Based Nanoplatelets as Active Materials for Electrochemical Double Layer Capacitors: A Comparative Study. Journal of The Electrochemical Society, 162 (1), A44–A51. doi: https://doi.org/10.1149/2.0381501jes
73. Chernysh, O. V., Khomenko, V. H., Barsukov, V. Z. (2016). Vplyv morfolohii poverkhni aliuminiievoho strumovidvodu na adheziiu elektrodnoho materialu i opir elektrokhimichnoho kondensatora. Visnyk KNUTD, 6, 188–194.
74. Borshch, A. V., Chernysh, O. V. (2015). Doslidzhennia nadiinosti kontaktu robochoi masy superkondensatora do metalevoho strumovidvodu. Naukovi rozrobky molodi na suchasnomu etapi, 1, 316.
75. Khomenko, V., Barsukov, V., Chernysh, O., Makyeyeva, I., Isikli, S., Gauthy, F. (2016). Green Alternative binders for high-voltage electrochemical capacitors. IOP Conference Series: Materials Science and Engineering, 111, 012025. doi: https://doi.org/10.1088/1757-899x/111/1/012025
76. Chernysh, O. V., Khomenko, V. H., Makieieva, I. S., Barsukov, V. Z. (2015). Vodorozchynni polimerni kompozytsii dlia khimichnykh dzherel strumu. Perspektyvni polimerni materialy ta tekhnolohii. Kyiv, 101–106.

77. Barsukov, V., Khomenko, V., Chernysh, O. et al. (2015). Green alternative binders for high voltage electrochemical capacitors and lithium-ion batteries. Baltic Polymer Symposium. Sigulda, 35.
78. Barsukov, V. Z., Khomenko, V. G., Senik, I. V., Chernysh, O. V. (2013). Litievye batarei dlia primeneniia na transporte: sovremennye problemy i perspektivy. Voprosy khimii i khimicheskoi tekhnologi, 4, 127–131.
79. Khomenko, V., Barsukov, V., Chernysh, O. et al. (2015). Development of Advanced Lithium-Ion Capacitors. 6th International Conference on Carbon for Energy Storage, Conversion and Environment Protection "CESEP' 2015". Poznan, 64.